Biochemical Pharmacology 83 (2012) 1393–1412

Contents lists available at SciVerse ScienceDirect

Biochemical Pharmacology

journal homepage: www.elsevier.com/locate/biochempharm

Cannabinoid receptor trafficking in peripheral cells is dynamically regulated by a binary biochemical switch

Jonas Kleyer [a], Simon Nicolussi [a], Peter Taylor [a], Deborah Simonelli [a], Evelyne Furger [b], Pascale Anderle [a], Jürg Gertsch [a,*]

[a] Institute of Biochemistry and Molecular Medicine, Swiss National Centre of Competence in Research NCCR TransCure, University of Bern, Bühlstrasse 28, CH-3012 Bern, Switzerland
[b] Institute of Pharmaceutical Sciences, ETH Zürich, Wolfgang-Pauli-Strasse 10, CH-8057 Zurich, Switzerland

ARTICLE INFO

Article history:
Received 18 January 2012
Accepted 17 February 2012
Available online 24 February 2012

Keywords:
Cannabinoid receptors
GPCR heterodimerization
Endocannabinoid system
Immune cells
Receptor trafficking

ABSTRACT

The cannabinoid G protein-coupled receptors (GPCRs) CB_1 and CB_2 are expressed in different peripheral cells. Localization of GPCRs in the cell membrane determines signaling via G protein pathways. Here we show that unlike in transfected cells, CB receptors in cell lines and primary human cells are not internalized upon agonist interaction, but move between cytoplasm and cell membranes by ligand-independent trafficking mechanisms. Even though CB receptors are expressed in many cells of peripheral origin they are not always localized in the cell membrane and in most cancer cell lines the ratios between CB_1 and CB_2 receptor gene and surface expression vary significantly. In contrast, CB receptor cell surface expression in HL60 cells is subject to significant oscillations and CB_2 receptors form oligomers and heterodimers with CB_1 receptors, showing synchronized surface expression, localization and trafficking. We show that hydrogen peroxide and other nonspecific protein tyrosine phosphatase inhibitors (TPIs) such as phenylarsine oxide trigger both CB_2 receptor internalization and externalization, depending on receptor localization. Phorbol ester-mediated internalization of CB receptors can be inhibited via this switch. In primary human immune cells hydrogen peroxide and other TPIs lead to a robust internalization of CB receptors in monocytes and an externalization in T cells. This study describes, for the first time, the dynamic nature of CB receptor trafficking in the context of a biochemical switch, which may have implications for studies on the cell-type specific effects of cannabinoids and our understanding of the regulation of CB receptor cell surface expression.

1. Introduction

The endocannabinoid system (ECS) consists of arachidonic acid-derived endocannabinoids including 2-arachidonoylglycerol (2-AG) and anandamide (AEA) which activate the cannabinoid G protein-coupled receptors (GPCRs) CB_1 and CB_2 [1]. While transport, synthesis and breakdown of endocannabinoids critically regulate endocannabinoid action, the degree of CB receptor surface expression can directly determine receptor function because CB receptors are known to signal via cell membrane associated $G_{\alpha i}$ pathways [2]. An increasing body of evidence implicates a role of the ECS in a variety of physiological and pathophysiological conditions, including immunomodulation, metabolic regulation, bone growth, pain, cancer, and psychiatric disorders [3–9], thus predisposing cannabinoid receptors as actual and potential therapeutic targets. Although CB_1 receptors are mainly expressed in the CNS [10], being responsible for the central effects of CB_1 receptor agonists, they are also co-expressed with CB_2 receptors in numerous peripheral cells such as immune cells, bone cells, keratinocytes, adipocytes, and renal tissue [11–15]. The type-2 (CB_2) receptors are predominantly expressed in peripheral cells,

Abbreviations: ATTC, American type culture collection; AMAM, anilino-monoindolylmaleimide; CB_1, cannabinoid receptor type-1; CB_2, cannabinoid receptor type-2; CDx, cluster of differentiation x; CHO, Chinese hamster ovary-K1; CM, cell membrane; CNR1, CB_1 receptor gene; CNR2, CB_2 receptor gene; DCA, dichloroacetate; DMEM, Dulbecco's modified eagle medium; DMSZ, German collection of microorganisms and cell cultures; DTSSP, 3,3′-dithiobis(sulfosuccinimidyl propionate); ECS, endocannabinoid system; ER, endoplasmic reticulum; FACS, fluorescence-activated cell sorting; FBS, fetal bovine serum; GRK, G protein receptor kinase; GPCR, G protein-coupled receptor; HEK, human embryonic kidney-293; H_2O_2, hydrogen peroxide; MCSF, macrophage colony stimulating factor; MCD, methyl-β-cyclodextrin; PAO, phenylarsine oxide; PBMCs, peripheral blood mononuclear cells; PBS-T, PBS with 0.01% Tween twenty; PDI, protein disulfide isomerase; PFA, paraformaldehyde; PKC, protein kinase C; PMA, phrobol 12-myristate 13-acetate; PTK, protein tyrosine kinase; PTP, protein tyrosine phosphatase; RT, room temperature; SFM, serum-free media; TPI, protein tyrosine phosphatase inhibitor; TBS, tris-buffered saline.

* Corresponding author at: Institute of Biochemistry and Molecular Medicine, NCCR TransCure, University of Bern, Bühlstrasse 28, CH-3012 Bern, Switzerland. Tel.: +41 31 631 41 24.
E-mail addresses: gertsch@ibmm.unibe.ch, juerg.gertsch@mci.unibe.ch (J. Gertsch).

0006-2952/$ – see front matter © 2012 Elsevier Inc. All rights reserved.
doi:10.1016/j.bcp.2012.02.014

including immune cells, with only minor expression levels in the CNS under normal conditions [16,17]. CB_2 receptors are known to be involved in immunomodulatory mechanisms that regulate inflammation [18]. The pharmacology of cannabinoids and cannabinomimetics, which selectively target CB receptors in peripheral tissues, is receiving increasing interest due to the tissue protective, metabolism regulatory and analgesic properties of these agents [19,20].

GPCRs are among the most common targets for pharmacological intervention in allopathic medicine [21]. GPCR ligands (agonists, protean agonists, inverse agonists, silent antagonists) typically bind to the receptor at the cell membrane and thereby alter the interactions of the GPCR with its downstream G protein effectors, thus modulating receptor signaling. Therefore, the number of receptors available for ligand interaction at the cell surface likely determines the overall responsiveness of a given cell type to drug treatment [22]. Based on these considerations, several previous studies have addressed CB_1 receptor trafficking and agonist induced internalization in some detail [23–26]. However, to date only limited data are available on CB_2 receptor trafficking and few studies have been carried out with primary cells [26]. Previous studies report phosphorylation of CB_2 receptors upon agonist stimulation [27,28] with subsequent receptor internalization [27,29–32]. Alternate stimulation of CB_2 receptors with agonists and antagonists has been shown to result in a pattern of repeated phosphorylation and dephosphorylation of the receptor, implicating the possibility of CB_2 receptor recycling [27]. Most of these studies have been carried out using transfected CHO-K1 or HEK293 cells with both tagged and non-tagged receptors. In GPCR research it is well established that assays using such cellular constructs show a pronounced internalization of GPCRs upon activation by agonists [33]. Although transfected cell lines provide excellent tools to study receptor localization and trafficking, according to the text-book paradigm of ligand-activated internalization [34,35], they may not necessarily reflect trafficking mechanisms as they occur under physiological conditions. Despite an increasing number of studies on cannabinoid receptor expression changes in pathophysiological conditions, the underlying mechanisms are only just beginning to unfold [22].

In the present study we demonstrate that CB receptors, with a focus on CB_2, apparently do not undergo agonist-induced internalization in different cell lines and primary peripheral human cells evaluated here, contrasting with data obtained from cell lines showing heterologous CB receptor overexpression. Furthermore, in human immune cells we describe an intrinsic ligand-independent trafficking mechanism, which is regulated by protein tyrosine phosphatases (PTPs). The protein tyrosine phosphatase inhibitor (TPI) phenylarsine oxide (PAO) was identified as a novel tool agent able to manipulate CB receptor surface expression bidirectionally. Applying PAO we uncovered an apparently physiological binary switch that externalizes or internalizes CB receptors in immune cells. The TPI hydrogen peroxide (H_2O_2), which is present during inflammation [36], activates the switch leading to a bidirectional trafficking between the cell surface and yet unidentified cytoplasmic compartments. Furthermore, for the first time we provide experimental evidence for endogenous heterodimer formation between CB_1 and CB_2 receptors in cell membranes of untransfected HL60 cells and portray and discuss the unexpectedly dynamic nature of CB receptor surface expression in these cells.

2. Materials and methods

2.1. Cell culture, PBMC isolation

HL60 cells (ATCC CCL-240) were cultured in Iscove's Modified Dulbecco's Medium (ATCC) supplemented with 20% FBS, penicillin, streptomycin and amphotericin B (all from Sigma–Aldrich, Switzerland) at 37 °C and 5% CO_2. NIH3T3 cells (ATCC CRL-2795) stably transfected with N-terminal eGFP tagged murine CB_2 receptor and CHO cells stably expressing human CB_2 were cultured in RPMI 1640 (Gibco) supplemented with 10% FBS, penicillin, streptomycin, amphotericin B and 400 μg/ml G418. Peripheral blood monocytes/macrophages and lymphocytes were isolated from buffy coat by density centrifugation according to a modified protocol by de Almeida et al. [37]. PBMC were isolated from buffy coats obtained from healthy blood donors by density gradient centrifugation. In a first step, buffy coat was mixed 1:1 with pre-warmed PBS and layered on top of a Ficoll cushion adjusted to a density of 1.070 g/ml by adding 2.813 ml PBS to 60 ml Ficoll Paque™ Premium (GE Healthcare, WI, USA) and then centrifuged for 30 min at 400 × *g* at RT. PBMCs were collected from the interface, washed three times with PBS–citrate buffer (1.49 mM disodium–dihydrogen–phosphate ($Na_2H_2PO_4$, Sigma–Aldrich, Switzerland); 9.15 mM disodium–phosphate (Na_2HPO_4, Sigma–Aldrich, Switzerland)); 139.97 mM sodiumchloride (NaCl), 13 mM trisodium citrate ($C_6H_5Na_3O_7$, Axon Lab, CH); pH 7.2) by centrifugation for 15 min at 100 × *g* and RT to remove platelets. For further purification, a two-step procedure with single gradients in each step was used. PBMCs were incubated for 15–30 min at 37 °C and 5% CO_2 in 15 ml of a solution with nine parts RPMI 1640 growth medium supplemented with 15 mM HEPES, 10% FBS and one part of 3.8% (w/v) trisodium citrate in PBS in 50 ml conical polypropylene tubes with loose tops in a CO_2 incubator. The two step Percoll (GE Healthcare, WI, USA) gradient was prepared in 50 ml polypropylene tubes with 9:11 Percoll lower phase (5 ml per tube; 9 parts PBS–citrate buffer and 11 parts isoosmotic Percoll with a final density of 1.093 g/ml) overlaid by a 1:1 Percoll phase (15 ml per tube; 1 part PBS–citrate buffer and 1 part isoosmotic Percoll with a final density of 1.064 g/ml). Isoosmotic Percoll for the gradient was prepared by adjusting Percoll to a density of 1.130 mg/ml with PBS then adding 10% (v/v) 1.5 M NaCl, resulting in a final density of 1.1228 mg/ml. The PBMC suspension was carefully layered on top of the two step Percoll gradient and centrifuged for 40 min at 400 × *g* and RT. Purified monocytes formed a discrete layer at the 11:9 and 1:1 Percoll interface and were collected with an average purity of 80–90% monocytes/macrophages and 10–20% lymphocytes as determined by flow cytometry. The cells beneath the monocyte/macrophage layer were also collected, consisting of a 1:1 mixture of monocytes/macrophages and lymphocytes in the middle and 95% pure lymphocytes toward the bottom. These PBMCs were stored frozen in liquid nitrogen until usage.

2.2. shRNA transfection experiments

Stable shRNA knockdown of CNR1 was performed by transfection of HL60 cells with Mission® Lentiviral Transduction Particles (Sigma–Aldrich, Switzerland) containing validated clones for CNR1 knockdown according to the manufacturer's instructions. Briefly, HL60 cells (100 μl) were plated in 96 well format at a density of 5×10^5 cells/ml in normal growth medium containing 8 μg/ml hexadimethrine bromide (Sigma–Aldrich; transfection medium). Mission® Lentiviral Particles containing shRNA for CNR1 or mock vector were added to the cells at a Multiplicity of Infection (MOI) of 5 and cells were subsequently spun down for 1 min at 800 × *g* and then incubated 2 h at 37 °C and 5% CO_2 for transfection. Cells were then centrifuged for 10 min at 800 × *g* before 75 μl of transfection medium was removed and substituted with 75 μl of normal growth medium. Cells were incubated at 37 °C and 5% CO_2 for 24 h to allow for antibiotic resistance gene expression, before addition of the selection antibiotic puromycin (2 μg/ml; Sigma–Aldrich, Switzerland)) was added. Three days later viable transfected cells

were transferred to 24 well plates for further propagation and CNR1 knockdown was monitored by CB_1 receptor surface expression by analytical FACS. The puromycin concentration was maintained at a concentration of 2 μg/ml for a total of 14 days for stable clone selection.

2.3. Assessment of CB receptor surface expression

For flow cytometric analysis of primary cells PBMC's were thawed, washed once with pre-warmed RPMI for DMSO removal of freezing medium and subsequently maintained in RPMI 1640 (Gibco) supplemented with 10% FBS and penicillin, streptomycin and amphotericin B at 37 °C and 5% CO_2 for compound treatment. HL60, U937 (CRL-1593.2) (myeloid), MCF7 (breast cancer), A549 (lung adenocarcinoma), Hela (CCL-2) (cervical cancer), PC3 (prostate cancer) and Caco-2 (colon carcinoma) cells were obtained from ATCC and grown in RPMI 1640 (Gibco) supplemented with 10% FBS and penicillin, streptomycin and amphotericin B at 37 °C and 5% CO_2. Importantly, primary monocytes started to differentiate immediately upon incubation with medium and the effects of PAO changed dramatically with differentiation state. Whenever cells were incubated with compounds to modulate CB receptor cell surface expression, possible cytotoxicity of the compound was excluded by Trypan Blue (Sigma–Aldrich, Switzerland) staining. CB_2 receptor cell surface expression levels of vehicle control cells was set to 100% (basal expression) and trafficking of receptor due to compound treatment was quantified in relation to this basal expression level. For immunostaining, cells were incubated on ice for 30 min with primary antibody (CB_1, Abcam 3558; CB_2, Abcam 3560) diluted in wash buffer (PBS, 2% FBS, 0.1% sodiumazide), washed twice with wash buffer containing primary antibodies, then incubated on ice with Fab-fragment Alexa Fluor® 488 secondary antibody (Invitrogen A11070) for 30 min in the dark. Fluorescence stained cells were washed twice, fixed with 1% p-formaldehyde in wash buffer and analyzed for antigen surface expression by analytical FACS (FACScan, Becton-Dickinson) using Cell Quest Pro (Becton-Dickinson) for data analysis. Unspecific binding of antibody to Fc receptors in immune cells was determined by incubation with rabbit IgG_1 antibody (Jackson-ImmunoResearch, 011-000-003), the corresponding IgG class used for primary antibody stain, and substracted from the obtained fluorescence values. Subpopulation staining of PBMCs was carried out by using specific CD3, CD4, CD8a, CD14, CD16 and CD19 antibodies either prelabeled with CE/Cy5 or stained with PE labeled secondary antibody (see Section 2.10).

2.4. CNR1 and CNR2 expression data analysis

Expression data for the NCI60 cell line panel was obtained through http://discover.nci.nih.gov/cellminer/ [38]. Robust multi-array averaging (RMA) and quantile normalization were used to quantify gene expression using the affy package (R, Bioconductor). Heatmaps were generated using Cluster 3.0 and TreeView (http://rana.lbl.gov/EisenSoftware.html) [39]. Centered correlation and average linkage clustering were used for similarity measurement and clustering, respectively.

2.5. Synchronization of HL60 cells by double-thymidine block

HL-60 cells were incubated for 24 h in medium containing 2 mM thymidine (Sigma–Aldrich, Switzerland) and then washed and resuspended in thymidine-free medium for 10 h. They were then again blocked by incubation with thymidine for 16 h. Release from the block was obtained by resuspension and cultivation in fresh RPMI-1640 medium 10% FBS without thymidine and penicillin, streptomycin and amphotericin B at 37 °C and 5% CO_2. The rate of synchrony achieved was monitored by removing aliquots of cultures at 60 min intervals for determination of DNA synthesis (Ml vs. G2M) and cell number by PI staining by FACS. In addition, DNA synthesis was determined by incorporation of [^{3}H]thymidine. Cells were incubated at a concentration of 2×10^5/ml with [^{3}H]thymidine (3 μCi/ml; specific activity, 5 Ci/ml) for 30 min at 37 °C. They were then washed and precipitated with 10% trichloroacetic acid; the precipitate was collected on Millipore filters, washed with 5% trichloroacetic acid, and counted in a Packard liquid scintillation counter. The Ml vs. G2M cell populations were determined by analytical FACS as published previously [40].

2.6. T cell activation

T cells were activated by incubation with soluble anti-CD3 (5 μg/ml) and anti-CD28 (2.5 μg/ml) antibody for 19 h followed by drug treatment for modulation of CB surface expression as adopted from a previously published protocol [41].

2.7. Cell membrane and lipid raft purification

The method for highly purified cell membrane (CM) preparation via aqueous two phase centrifugation was adapted from Park et al. [42]. All steps were carried out on ice or at 4 °C. 1–3 × 10^7 HL60 cells were pelleted by centrifugation and washed 1× with PBS. The pellet was resuspended in 1.5 ml lysis buffer (15 mM Tris pH 7.5, 250 mM sucrose, 2 mM $MgCl_2$, 1 mM EDTA, 1 mM DTT, 1 mM sodium fluoride, 1 mM sodium orthovanadate and protease inhibitor cocktail from Sigma–Aldrich, Switzerland (P8340)) and then homogenized in a Dounce homogenizer with 50 strokes using a tight fitting pestle B. The cell lysate was then centrifuged for 10 min at 1000 × *g* and 4 °C to remove nuclei and cell debris. Supernatant was recovered and the remaining pellet resuspended in 2 ml lysis buffer for an additional centrifugation under the same conditions. Supernatants from the first and second centrifugation were pooled (post nuclear CM fraction), layered onto a 30% Percoll (w/v) cushion and centrifuged at 84,000 × *g* for 35 min at 4 °C in a TST 41.14 rotor (Beckman). The purified CM forming a visible cloudy layer at the interface between the lysis buffer and Percoll cushion was collected by punctuation of the ultracentrifuge tube with a 26 gauge needle and withdrawal of the cloudy interface (approximately 1 ml). Further aqueous two-phase extraction of CM was carried out following the protocol of Park et al. [42] by preparing two sets of a 6.6% (w/w) Dextran 500 gradient/6.6%, (w/w) polyethylene glycol 3350 (PEG, Sigma–Aldrich, Switzerland) via the addition of stock solutions of 20% (w/w) Dextran 500 (Roth, Germany) and 40% (w/w) PEG 3350. Crude CM sample was added into one set of the two-phase mixtures. The potassium phosphate buffer (0.2 M, pH 7.2) was added to the other set of two-phase mixtures. After 40 inversions at 4 °C, the two phase mixtures were centrifuged for 5 min at 750 × *g* and 4 °C. Subsequently the two-phase mixtures were phase-separated via centrifugation, forming two phases with PEG in the upper phase and Dextran in the lower phase. The two upper phases of the two-phase systems were exchanged. The mixtures were inverted 40 times at 4 °C and subjected to another centrifugation for 5 min at 750 × *g* and 4 °C. The two upper phases were recovered, pooled and centrifuged for 2 h at 100,000 × *g* with 1 mM sodium bicarbonate according to Cao et al. [43]. The purified CM formed a pellet after centrifugation, which after removal of the supernatant was resuspended in Co-IP buffer for immunoprecipitation. Lipid rafts were prepared as described by Yamazaki et al. [44] with slight modifications. All steps were carried out at 4 °C or on ice. Cells were incubated in 1 ml TNE buffer (25 mM Tris base, 150 mM NaCl, 5 mM EDTA, protease inhibitor solution (Sigma–Aldrich, Switzerland, pH 7.4) containing 1% Triton X-100 for 30 min on ice followed by homogenization in a Dounce homogenizer with 30 strokes. Cells were then centrifuged for 5 min at 1500 × *g* to remove nuclei and

cell debris. The supernatant was collected and diluted 1:1 with 80% sucrose in TNE buffer, resulting in a final sucrose concentration of 40% with a volume of approximately 1.8 ml, and transferred to an ultracentrifuge tube. The homogenate was overlaid with sucrose solution in TNE buffer of varying concentrations (2 ml 30% sucrose and 1 ml 5% sucrose on top of the gradient) and centrifuged for 19 h at 250,000 rcf in a Beckman SW55Ti rotor at 4 °C. A light scattering band at the 5% and 30% sucrose interface corresponded to the lipid raft fraction. Fractions of 400 μl were collected from the top of the tube with fractions 3–5 containing the isolated rafts. Surface proteins of 4×10^7 HL60 cells were cross-linked with 1.9 mM DTSSP (Pierce) according to manufacturer's instructions before lipid rafts were isolated for immunoprecipitation.

2.8. Co-immunoprecipitation and Western blotting

The co-immunoprecipitation of CB_1 and CB_2 receptors from purified HL60 cell membranes was carried out using Dynabeads G (Invitrogen, CA, USA) according to the manufacturer's instructions. Two different antibodies for CB_1 (Sigma–Aldrich, Switzerland C1108, epitope aa 1–99 hCB1; Abcam ab3558, epitope aa 1–99 hCB_1) and CB_2 (Sigma–Aldrich, Switzerland C1483, epitope aa 1–32 rCB2; Abcam ab3560, epitope aa 1–33 hCB_2) were used for precipitation. Briefly, 3 μl anti-CB_1 or anti-CB_2 antibody and 4 μl anti-p38 antibody (negative control) were diluted 1:10 in citrate phosphate buffer pH 5.0 (25 mM citrate, 50 mM disodium phosphate) and incubated with 30 μl magnetic beads for 20 min at RT with gentle tilt and rotation. After three wash steps, antibodies were immobilized on beads by incubation with 5 mM BS^3 (Pierce Thermo Scientific, IL, USA) for 30 min. Subsequently beads were incubated with 100 μl isolated cell membrane for antigen capture for 40 min at 4 °C with gentle rotation. Beads with captured antigen were washed 3 times with PBS pH 7.4 followed by mild antigen elution with 2×20 μl glycin pH 2.6. LDS (4×) was added to reach the final concentration (1×) before samples were boiled for 5 min at 95 °C. Samples were then electrophoresed on NuPage® (Invitrogen) precast 4–12% gradient gels and transferred to nitrocellulose membrane. The Fermentas pre-stained marker (Page Ruler Plus) was run alongside the samples. Membranes were blocked with 5% non-fat milk in PBS with 0.01% Tween 20 (PBS-T) overnight, briefly rinsed twice with PBS-T, then incubated with either CB_1 (Abcam) or CB_2 (Abcam) antibody diluted 1:250 in PBS-T for 1 h at RT. After 3 washes with PBS-T for 15 min membranes were incubated with horseradish peroxidase-conjugated sheep anti-rabbit antibody (GE Healthcare) diluted 1:2000 in PBS-T for 1 h at RT. Following three further washes, membranes were incubated with ECL-plus (GE Healthcare) for 1 min for signal detection on autoradiographic SuperRX film (Fujifilm). To study the potential degradation of the PMA internalized CB2 receptors, 0.5×10^6 HL60 cells per sample were stimulated with 50 nM PMA, harvested at indicated times and subsequently lysed in RIPA buffer (50 mM Tris, 150 mM NaCl, 0.1%SDS, 0.5% sodium deoxycholate, 1% Triton X 100, protease inhibitor cocktail (P8340), all from Sigma–Aldrich, Switzerland). Cells were incubated 30 min on ice for lysis and subsequently centrifuged 15 min at $15{,}000 \times g$ at 4 °C. The supernatant was harvested and the protein concentration was determined with Pierce BCA Protein Assay Kit (23225, Thermo Scientific, USA), before equal amounts of protein were loaded on NuPage® (Invitrogen) precast 4–12% gradient gels. Detection of antigen was carried out as described above, using the antibodies Proliferating Cell Nuclear Antigen (PCNA, 307901, Biolegend, USA) as loading control and CB_2 receptor (Abcam 3560).

2.9. Microscopy

NIH3T3 cells stably transfected with N-terminal eGFP tagged murine CB_2 receptor (NIH3T3-CB_2-GFP) were incubated with Lysotracker® and Mitotracker® (both Invitrogen, Switzerland) according to the manufacturer's instructions. Briefly, cells were incubated with 50 nM Lysotracker® for 30 min in normal growth medium and with 50 nM Mitotracker® for 15 min in FBS free RPMI 1640 medium. Cells were subsequently washed twice with PBS and fixed with PFA before images were immediately acquired. For immunostaining of endoplasmatic reticulum and early endosomes, NIH3T3-CB_2-GFP cells were fixed in 4% paraformaldehyde in PBS for 10 min, permeabilized with 0.05% Triton X-100 in PBS for 3 min and blocked with 0.5% BSA and 10% goat serum in PBS for 1 h at RT. Fixed monolayers were incubated with primary antibodies against Early Endosome Antigen 1 (EEA1, BD Biosciences) for endosome staining and Protein Disulfide Isomerase (PDI, Stessgen) diluted 1:500 in 0.5% BSA and 5% goat serum (Sigma–Aldrich, Switzerland) for 90 min. Then, after 3 washes with PBS, cells were incubated with appropriate Alexa 594-conjugated secondary antibody (A11020, Invitrogen) for 1 h at RT. 3 washes with PBS, images from fixed and stained monolayers were obtained with a Nikon DS-Fi1 camera mounted on a Nikon Eclipse TS100 microscope equipped with a Tripleband DAPI/FITC/TRITC HC filterset (AHF, Germany).

2.10. Antibodies and reagents

Unless stated otherwise, chemicals were obtained from Sigma–Aldrich, Switzerland. Anandamide, 2-arachidonoylglycerol and CP,55,940 were purchased from Tocris (MO, USA) and BPA-AM2 from Funakoshi (Tokyo, Japan). Mission® Lentiviral Transduction Particles for validated CNR1 knock down were obtained from Sigma–Aldrich, Switzerland (NM ID: NM_001840, clone TRCN000011282). Antibodies used for lymphocyte subpopulation stains were PE/Cy5 conjugated CD8a (Biolegend, 300909) and CD19 (Biolegend, 302209), PE conjugated CD4 (Sigma–Aldrich, Switzerland, P-7562) and unconjugated CD3 (Biolegend, 300313) and CD16 (Biolegend, 302013). Unconjugated antibodies were fluorescence labeled with R-PE labeled secondary antibody (Sigma–Aldrich, Switzerland, P-8547). Phorbol 12-myristate 13-acetate (PMA), 1-stearoyl-2-arachidonoyl-sn-glycerol (SAG), phenylarsine oxide, cyclosporin A (CsA), genistein, CD45-540215, insulin, methyl-β-cyclodextrin (MCD), sodium orthovanadate (Na_3VO_4), tumor necrosis factor-α (TNF-α), PD 166285 and AS 1949490 were all obtained from Sigma–Aldrich, Switzerland. Thapsigargin (THG) was purchased from Alexis Biochemicals, USA. Lipopolysaccharide (LPS), dexamethasone, H_2O_2, n-butanol and propranolol were purchased from Sigma–Aldrich, Switzerland. Macrophage colony-stimulating factor (MCSF) was from Abcam. NSC87877 and cantharidine was purchased from Tocris.

2.11. Microarray data and statistical analysis

Expression data for NCI60 cell line panel was obtained through http://discover.nci.nih.gov/cellminer/ [35]. Robust multi-array averaging and quantile normalization were used to quantify gene expression using the affy package (R, Bioconductor). Heatmaps were generated using Cluster 3.0 and TreeView (http://rana.lbl.gov/EisenSoftware.html [39], Cluster analysis and display of genome-wide expression patterns). Centered correlation and average linkage clustering, respectively, were used for similarity measurement and clustering. Statistical analysis was performed with Prism 5 (GraphPAD Software for Science, CA, USA) and R CRAN, applying unpaired Student's *t*-test, one-way and two-way ANOVA, and Tukey HSD for post hoc testing. For oscillations repeated measures ANOVA was employed. All statistical tests were two-sided and a p value or adj. p value, respectively, <0.05 was considered statistically significant.

3. Results

3.1. Agonist stimulation induces CB receptor internalization in stably-transfected CHOK1-hCB_2 and CHOK1-hCB_1 cells, but not in cell lines and primary peripheral immune cells

The majority of previous studies aimed at elucidating trafficking mechanisms of CB receptors have been carried out using overexpression cell lines, describing agonist-induced internalization for both CB_1 and CB_2 receptors [23,31,32]. To corroborate whether this would also occur in primary peripheral blood mononuclear cells (PBMCs) or peripheral cell lines we studied agonist-induced internalization of CB receptors. hCB_2 and hCB_1 receptor-transfected CHOK1 cells, isolated primary lymphocytes and monocytes/macrophages and HL60 cells were exposed to 10 μM of different agonists for 1 h and the receptor surface expression was quantified by analytical FACS. In agreement with previous reports [29–31], AEA, 2-AG and CP55,940 led to significant CB receptor internalization in CHO-hCB_2 and CHO-hCB_1 cells (Fig. 1A). We used selective polyclonal antibodies (Abs) to label the N-termini of CB receptors. Although the CB_2 receptor antibody used showed a higher non-specific binding (i.e. background) than the CB_1 receptor antibody, the Abs proved to be selective and were thus judged suitable to quantify receptor surface expression (Fig. 1B). Unexpectedly, neither primary PBMCs nor HL60 cells displayed CB receptor internalization upon exposure to agonists (Fig. 1C), suggesting that CB receptor trafficking in these cells may be regulated in an agonist-independent manner. The same results were obtained with the peripheral cell lines MCF7, A549 and Caco-2 (Fig. 1D), showing relatively weak overall CB_2 receptor surface expressions (see below). Notably, in none of many experiments performed on CB receptor surface expression with primary cells or non-transfected cell lines could we observe agonist-mediated internalization. This unexpected finding and the fact that CB receptor gene expression is often used as an indicator of functional CB receptor expression [45–48], led us to explore the relationship between CNR gene expression and localization of CB receptors in different cell types.

3.2. Lack of correlation between CNR gene expression and CB receptor surface expression and dynamic changes in the latter

Based on gene array data in the NCI60 cell line panel in most peripheral cells the CB_2 receptor gene (CNR2) is more strongly

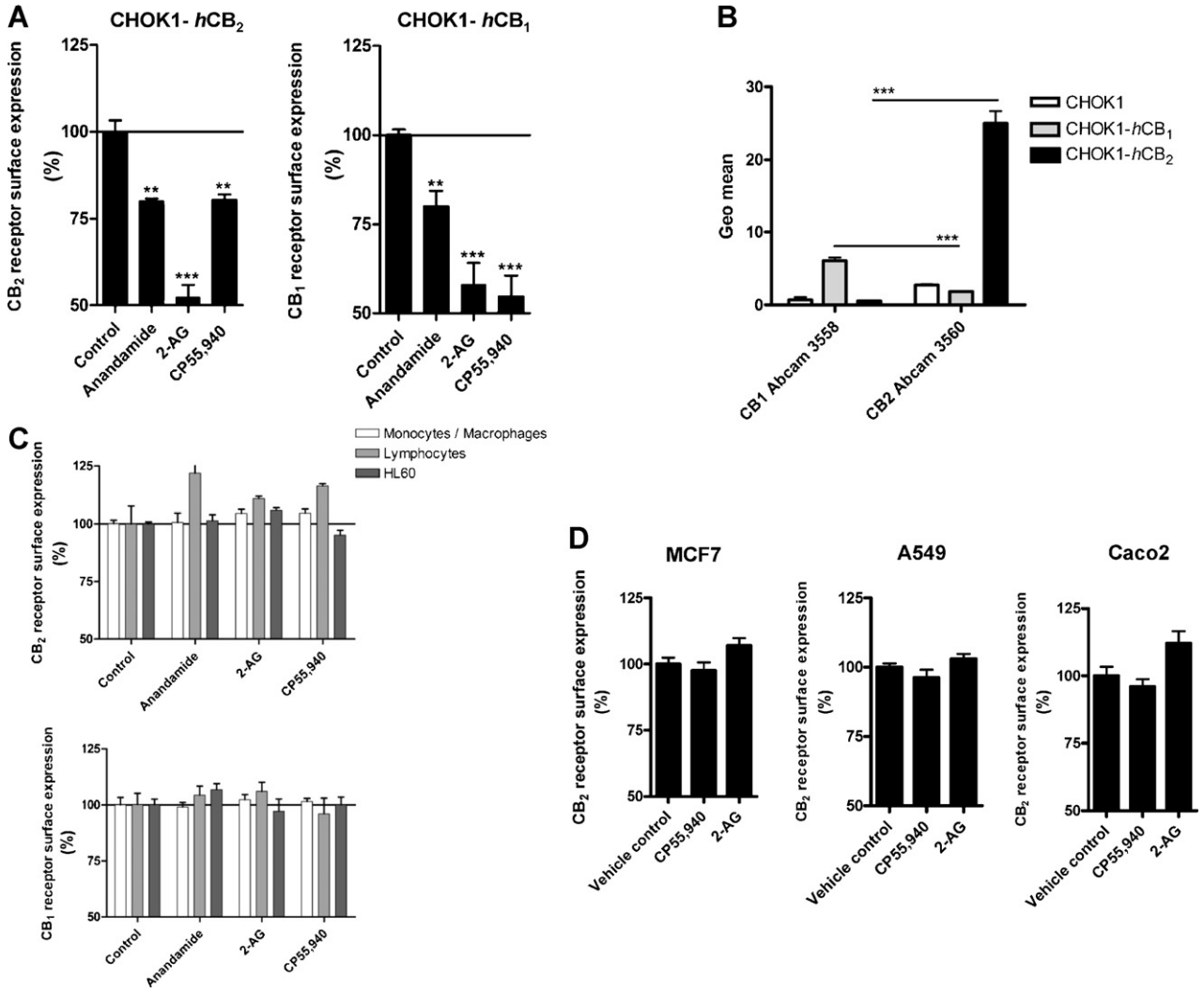

Fig. 1. Effect of agonist treatment on CB receptor cell surface expression (% of control) in transfected CHOK1 cells and peripheral cells. (A) CB receptor surface expression following agonist (10 μM) stimulation by anandamide, 2-AG and CP55,940 for 1 h in stably transfected hCB_1 and hCB_2 CHOK1 cells (1×10^6). (B) Selectivity of background staining of polyclonal Abs in CHOK1 cells transfected with either hCB_1 or hCB_2 receptors. (C) CB receptor surface expression in primary monocytes/macrophages and lymphocytes and HL60 cells. (D) CB_2 receptor surface expression in MCF7 (breast adenocarcinoma), A549 (lung adenocarcinoma) and Caco-2 (colon carcinoma) cells (1×10^6) after agonist (10 μM) stimulation for 1 h. At least 5×10^3 gated cells were quantified in analytical FACS experiments. Nonspecific binding to Fc receptors in immune cells was negligible. Data show mean values ± SD, $N = 3$. Data were analyzed using unpaired t-test, $^{**}p < 0.01$ and $^{***}p < 0.001$.

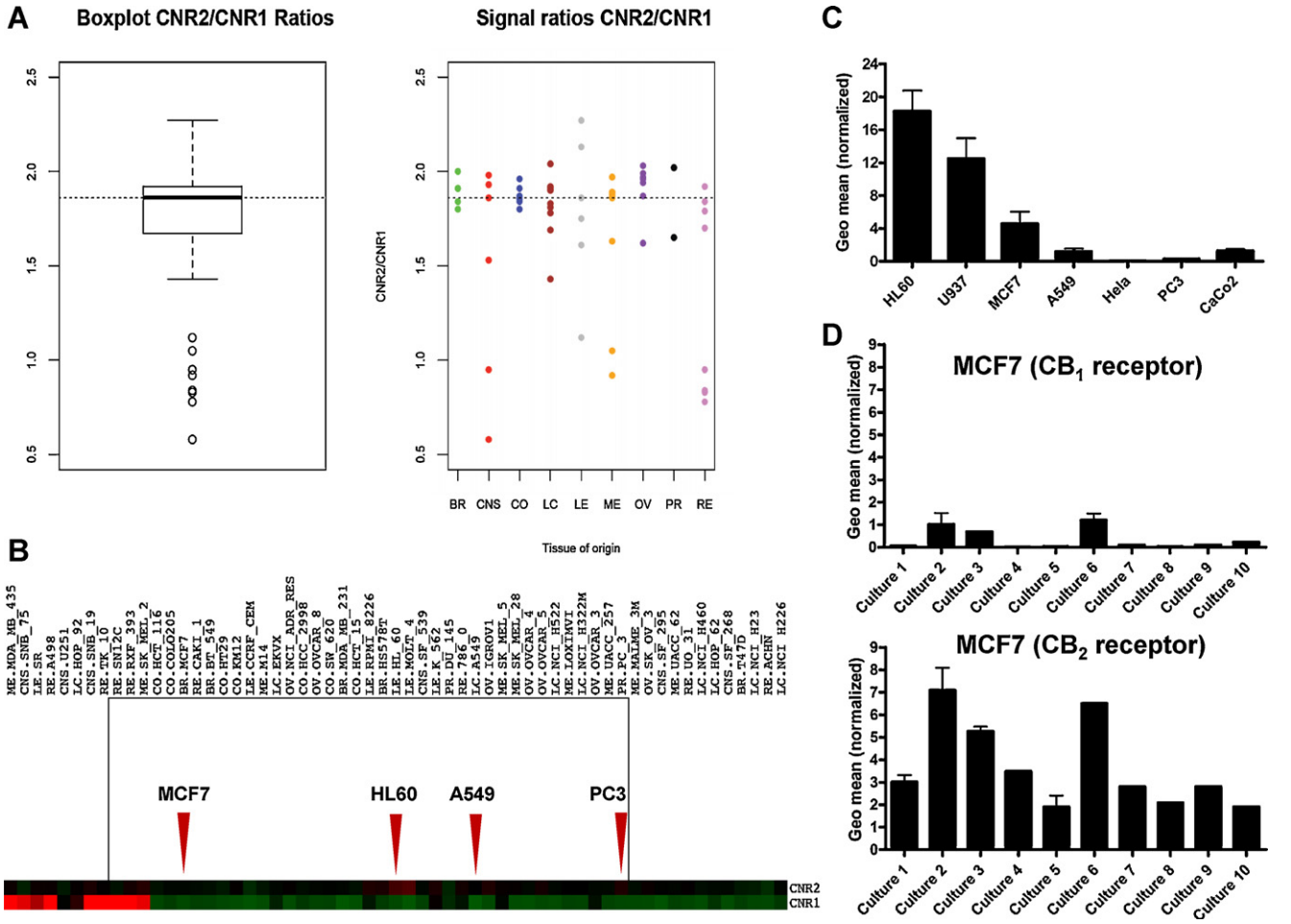

Fig. 2. (A) Expression profiles of the genes CNR1 and CNR2 in the NCI60 cell line panel. Boxplot of the signal ratios CNR2/CNR1 in all 59 cell lines (left). Normalized signal ratios in the various tissues represented in the NCI60 cell line panel: BR = breast, CNS = central nervous system, CO = colon, LC = lung, LE = leukocytes, ME = melanoma, OV = ovarian tissue, PR = prostate, RE = renal tissue (right). (B) Relative expression levels of CNR1 and CNR2 showing homogenous expression of CNR2 (colors are not absolute measured but relative to overall gene expression in cell line). (C) Differences of CB_2 receptor surface expression between distinct cell lines. (D) Significant fluctuations of CB_1 and CB_2 receptor surface expressions between different MCF7 cell culture experiments. Data were analyzed using a paired *t*-test. At least 5×10^3 gated cells were quantified in analytical FACS experiments. Data show mean values ± SD, $N = 3$. (For interpretation of the references to color in this figure legend, the reader is referred to the web version of the article.)

and more homogenously expressed than that of the CB_1 receptor (CNR1), as also indicated by the average CNR2/CNR1 expression ratio >1.5 (Fig. 2A and B). Certain cell lines of brain and renal origin are notable exceptions because they show stronger CB_1 receptor expressions relative to other genes (Fig. 2A). As shown in Fig. 2B, the CNR2 gene is most strongly expressed in HL60 cells (relative to background expression), from which this receptor was first cloned [49]. In order to check whether gene expression correlates with CB receptor surface expression, we measured CB receptor surface expression in U937 (myeloid), MCF7 (breast cancer), A549 (lung adenocarcinoma), Hela (cervical cancer), PC3 (prostate cancer) and Caco-2 (colon carcinoma) cells. As shown in Fig. 2C, Hela and PC3 cells showed no or only marginal CB_2 receptor surface expression. Moreover, several other cell lines which display significant CNR2 expression did not show any CB_2 receptor surface expression (data not shown), thus suggesting a cytoplasmic localization. In our study we found that different cell culture passages, or different clones from the same cell lines, showed significantly different CB receptor surface expression patterns (Fig. 2C and D). In Fig. 2D, CB receptor cell surface expression differed significantly between different experiments (i.e. different cell cultures) in MCF7 cells and also in HL60 cells (see below). Our data therefore suggest that there are intrinsic ligand-independent changes that mediate CB receptor surface expression. Because CB_2 receptors were generally more abundantly expressed at the cell surface than CB_1 receptors in peripheral cells, we focussed our study on trafficking mechanisms regulating CB_2 receptors.

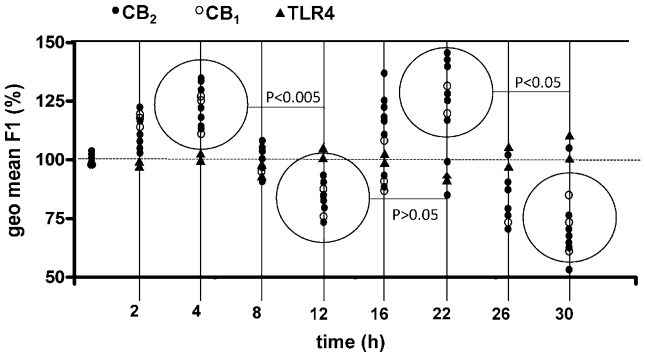

Fig. 3. Intrinsic oscillations of CB_2 and CB_1 receptor surface expression in synchronized HL60 (ATCC CCL-240) cells. 1×10^7 cells were synchronized by a double-thymidine block and surface expression of CB_2, CB_1 and TLR4 proteins were measured at different time points. 1×10^4 cells from the same population were quantified by analytical FACS. Data points show independent experiments ($N > 4$) and significant differences for relative geo mean values between indicated time points (circles) were determined by repeated measures ANOVA and Tukey post hoc analysis.

3.3. Intrinsic synchronous oscillations of CB receptors in HL60 cells and oligomer and heterodimer formation between CB_1 and CB_2 receptors

Promyelocytic HL60 cells (ATCC CCL-240) not only showed strong CNR1 and CNR2 gene expression (Fig. 2B) but also strong and relatively robust CB receptor cell surface expression. In contrast to other cell types, which preferentially expose only CB_2 receptors on their surface (see below), in HL60 cells both CB receptors were detected at similar levels. When HL60 cells were synchronized by a double-thymidine block, they revealed a type of synchronous oscillation of both CB receptors while such fluctuations were not seen with the toll-like receptor 4 (TLR4) (Fig. 3). Interestingly, CB_1 and CB_2 receptors oscillated in synchrony, indicating potential co-regulation. The overall changes were in the range of 100% relative to initial levels and statistically significant between certain time points as determined by Repeated Measures ANOVA (4 h vs. 12 h vs. 22 h). CB receptor surface expression did not correlate with cell cycle events (data not shown). Monitoring surface expression of CB_1 and CB_2 receptors in different experiments revealed significant fluctuations between clones from different suppliers (Fig. 4A), as well as passage numbers or culture conditions (Fig. 4B). We have previously reported on the HL60 clone 4 (Fig. 4B) which lacks CB receptor surface expression and does not respond to 2-AG stimulation [50]. Despite these differences between the HL60 clones, an apparently constant ratio of 1:1 for CB_1 and CB_2 receptors was measured, independent of the absolute surface expression (Fig. 4A and B). This observation led us to hypothesize that CB_1 and CB_2 receptors may form stable heterodimers in HL60 cells and that this could be the reason for the apparently synchronous cell surface expressions.

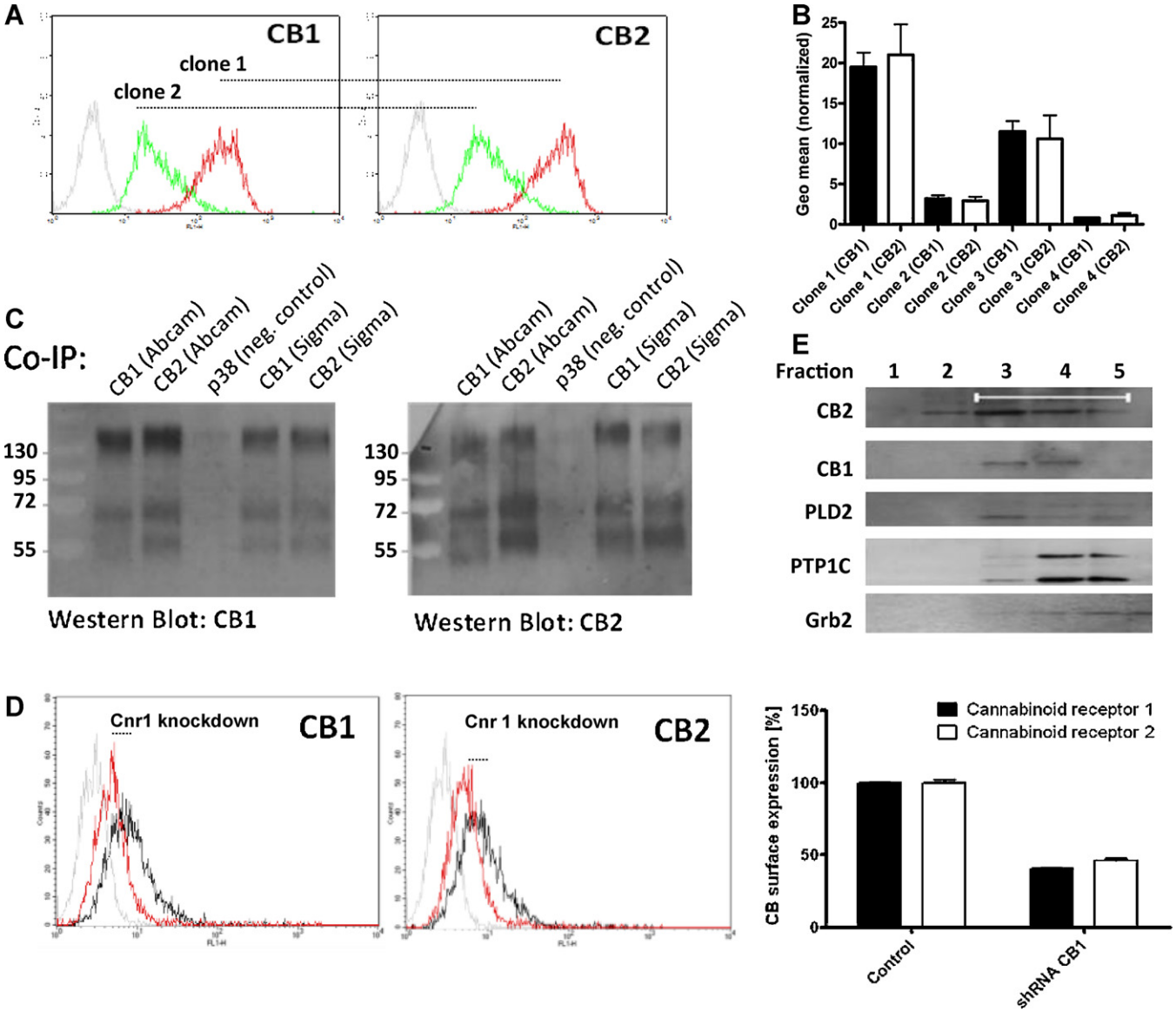

Fig. 4. CB_1 and CB_2 receptors form heterodimers and oligomers in untransfected HL60 cells (A) HL60 cell lines from certified batches of different suppliers; clone 1 (ATCC) and clone 2 (DSMZ) with significantly different basal CB receptor expressions. (B) Relative CB receptor surface expressions from different HL60 (ATCC) clones maintained in our laboratory. (C) Co-immunoprecipitation of CB_1 and CB_2 receptors from purified cell membrane fractions of HL60 cells, using two different antibodies for each CB receptor (Abcam and Sigma, all antibodies with N-terminal epitope) and p38 as negative control for unspecific binding. Double bands at approximately 60 kDa likely show nonglycosylated vs. glycosylsated monomers of the CB receptors. At approximately 160 kDa higher order oligomeric complexes of trimeric or tetrameric composition are detected as previously reported [20]. (D) shRNA knockdown of CNR1 decreased CB_1 receptor surface expression to ~40% of the mock transfected control, resulting in a stoichiometrically matching decrease (~46% of control) of CB_2 receptor surface expression. (E) Western blot analysis of HL60 lipid raft preparation. Both CB_1 and CB_2 receptors are detected in the lipid raft fraction (lanes 3–5 on blot). Phospholipase D2 (PLD2), protein tyrosine phosphatase 1C (PTP1C) and growth factor receptor-bound protein 2 (Grb2) were used as positive controls for raft preparation. At least 5×10^3 gated cells were quantified in analytical FACS experiments. Data shown are mean values ± SD, $N = 3$.

Immunoprecipitation and co-immunoprecipitation experiments of CB_1 and CB_2 receptors from purified HL60 cell membranes, using two different Abs for each receptor, revealed that both CB_1 and CB_2 co-precipitated and apparently formed heterodimers and higher-order heterooligomers (Fig. 4C). As we wanted to avoid artificial co-localization of CB receptors due to overexpression, a membrane purification step was introduced (see Section 2) which was essential to detect the endogenously expressed CB receptors. The observed staining pattern of the antibodies for CB_1 receptors seen have been reported in a study by Wager-Miller et al. [51], showing both the monomeric and high molecular weight forms. As only the CB_1 receptor antibody was used, homo- or hetero-complex formation of the multimeric complex was not revealed in this report. To test whether the apparent heterodimer formation in HL60 cells, detected in the co-immunoprecipitation experiments, also affects the membrane localization (i.e. trafficking) of CB receptors in living cells, we made shRNA knockdown mutants of CNR1 from HL60 cells. Quantification of receptor surface expression after shRNA treatment showed a 60% reduction compared to the mock transfection control (Fig. 4D). Intriguingly, the reduction of CB_1 receptor surface expression was accompanied by a stoichometrically matching decrease in CB_2 receptor surface expression to approximately 46% of control levels, thus indirectly confirming heterodimerization and co-localization. To further characterize the membrane localization properties of CB receptors in the HL60 cell line, lipid rafts were prepared and analyzed by immunoblotting. Our data indicate the presence of both receptors in these compartments (Fig. 4E), despite the fact that only CB_1 receptors appear to have the biochemical properties that makes them reside in the lipid raft microdomains [52].

3.4. CB_2 receptor surface expression is controlled by protein tyrosine phosphatases—elucidation of a binary biochemical switch

In order to find a mechanistic basis for the oscillation and overall changes of the CB receptor surface expression observed, we next investigated which pharmacological agents (nonspecific modulators of kinases, calcium homeostasis, growth factors, etc.) were able to trigger CB_2 receptor trafficking (i.e. internalization and/or externalization). PBMCs were incubated with non-cytotoxic concentrations of the respective inhibitors (Fig. 5A). Monocyte/macrophage $CD14^+$ cell populations were gated and CB_2 receptor surface expression quantified by analytical FACS. The phorbol ester phorbol 12-myristate 13-acetate, which is a diacylglycerol mimic that binds to C1 domains in kinases including PKC [53] was determined to be highly active (Fig. 5A). PMA at 50 nM led to a rapid and maximal internalization of both CB receptors in cell lines and in primary human $CD14^+$ monocytes (Fig. 5B), equivalent to about 50% of the total detectable receptors. Although we are the first to describe this effect for CB receptors, PMA has previously been reported to modulate GPCR trafficking [54]. Using PMA as a trigger for CB receptor internalization we provide evidence that the CB_2 receptor-dependent intracellular calcium transients induced by 2-AG in HL60 cells [50] may be mediated by the fraction of CB_2 receptors that are internalized upon treatment (Fig. 5C). Thus, it is feasible that the pool of receptors that undergoes trafficking is functional and may be important for signal transduction, or alternatively, PMA shuts down the down-stream effects involved in the CB_2 receptor-mediated intracellular calcium transients. PMA treatment did not lead to degradation of the CB_2 receptor pool as illustrated by Western blot analyses carried out with HL60 cells and primary $CD14^+$ monocytes/macrophages (Fig. 5D). Confocal microscopy confirmed that surface CB_2 receptors are rapidly internalized upon PMA treatment (supplemental Fig. 1) in primary $CD14^+$ monocytes/macrophages. Interestingly, phenylarsine oxide, a nonspecific TPI [18], also significantly internalized CB_2 receptors in $CD14^+$ monocytes/macrophages (Fig. 5A). Importantly, this effect appeared to be dependent on the monocyte differentiation state and could even be reversed in differentiated macrophages (Fig. 5A). To elucidate the mechanism of PMA-induced CB receptor internalization we next screened a range of kinases and phosphatases inhibitors, in addition to other agents known to affect primary cellular mechanisms. Notably, the internalization triggered by PMA could not be blocked by staurosporine or anilino-monoindolylmaleimide (AMAM) (Fig. 6), which are used as nonspecific PKC and PKCβ inhibitors, respectively [55], clearly suggesting a PKC-independent mechanism. As shown in Fig. 6, during this screening we found that PAO, here shown to be a receptor internalizing agent (Fig. 5A), also effectively reversed the effect of PMA (Fig. 5A). Since PMA is nonspecific and exerts a broad range of effects, PAO is a broad-range TPI, and the phospholipase inhibitor n-butanol showed a tendency to externalize CB_2 receptors (Fig. 5A), we next tested a series of phosphatase, kinase and phospholipase D inhibitors. As shown in Fig. 6, none of the inhibitors but PAO was able to reverse the effect of PMA. Because PMA exerts a broad range of effects and other TPIs did not match the effect of PAO in this assay (data not shown), we did not continue this pursuit of combinatorial effects.

More interestingly, PAO was able to induce rapid CB receptor externalization in lymphocyte subsets that showed little or no constitutive CB_2 receptor surface expression. This effect was extremely robust (i.e. reproducible between individual blood donors) and thus enabled us to use PAO as a molecular tool to trigger CB receptor trafficking. To characterize the CB receptor trafficking in primary immune cells in more detail, subpopulations of lymphocytes were monitored for changes in surface expression after exposure to PAO. $CD3^+$, $CD4^+$ and $CD8a^+$ lymphocytes with low levels of basal CB_2 receptor expression (geo mean $\sim$ 3–5) displayed externalization of the receptor (Fig. 7A). In contrast, natural killer $CD16^+$ cells, which are the lymphocyte subpopulation with the highest (geo mean $\sim$ 200) basal CB_2 receptor expression [17], showed an internalization of the receptor (Fig. 7A), suggesting PAO was acting as a trigger for a binary biochemical switch. Interestingly, in $CD19^+$ B cells surface expression of CB_2 receptors did not change upon PAO treatment (Fig. 7A), indicating a differential mode of regulation in this cell type or a lack of robust CNR2 expression. In our search for natural TPIs which may trigger the externalization of CB receptors in lymphocytes we found that hydrogen peroxide (H_2O_2), which is an endogenous reversible inhibitor of PTPs present in inflammatory tissues and the tumor microenvironment [36,56], induces the same effect as PAO (Fig. 7B). It also triggered CB_2 receptor trafficking in $CD14^+$ monocytes/macrophages and lymphocytes. Peripheral blood mononuclear cells from different donors were exposed to increasing concentrations of H_2O_2, as well as in combination with orthovanadate, leading to the formation of pervanadate, which is an irreversible TPI [57]. The extent of PTP inhibition clearly correlated with the elicited trafficking response in a dose-dependent manner (Fig. 7B), resulting in CB_2 receptor internalization in $CD14^+$ monocytes/macrophages and CB_2 receptor externalization in lymphocytes. The bidirectional trafficking in response to TPI treatment was determined by the basal surface expression of the receptor prior to treatment and thus illustrates the binary nature of the biochemical switch.

HL60 cells with different levels of basal receptor expression (low and high; geo mean values $\sim$5 and $\sim$160) were treated with H_2O_2, resulting in the predicted differential trafficking response according to basal surface receptor levels (Fig. 7C). These results confirm the regulation of the trafficking response observed in primary cells. Fig. 7D illustrates the effect of 3 different TPIs on CB_2 receptor surface expression in monocytes/macrophages, lymphocytes and HL60 cells. The binary switch regulation of CB_2 receptor surface expression was seen with all three TPIs in the different cell types with high statistical significance ($p < 0.005$) except for BPA-AM_2 in monocytes/macro-

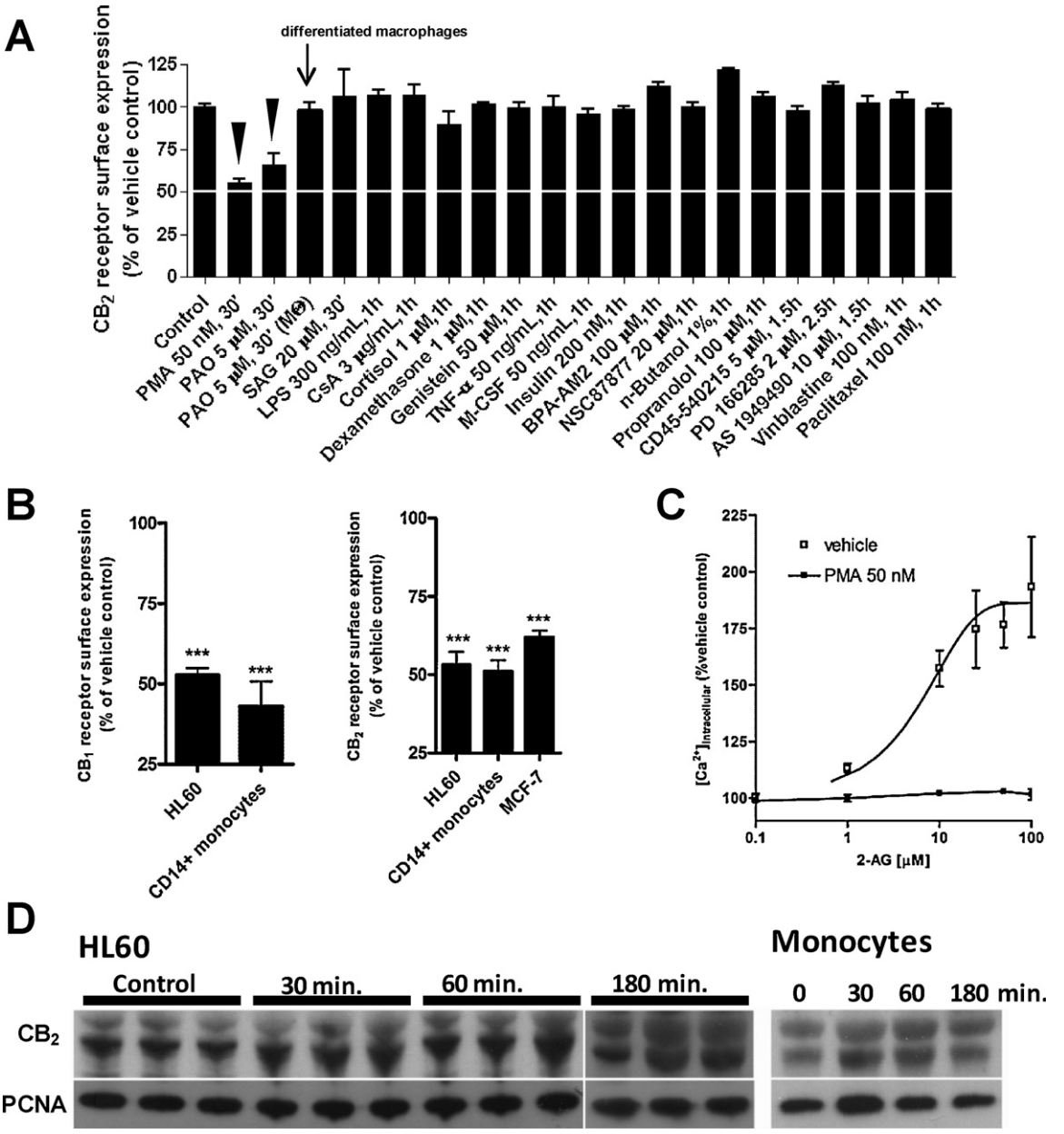

Fig. 5. Screening for agents that induce CB receptor internalization in CD14$^+$ monocytes/macrophages. (A) A screen of different non-specific inhibitors and modulators of cellular functions shows that PMA and PAO significantly internalize CB_2 receptors. (B) Both CB_1 and CB_2 receptors are internalized by 50 nM PMA (30 min) in HL60 cells, primary monocytes/macrophages and MCF7 cells (1×10^6). Data show mean values ± SD, $N = 3$ and were analyzed in a paired t-test. $^{***}p < 0.001$. (C) Pre-treatment by 50 nM PMA for 30 min abolishes 2-AG-induced intracellular calcium in HL60 cells. At least 5×10^3 gated cells were quantified in analytical FACS experiments. (D) CB_2 receptor Western blot showing a lack of protein degradation over 180 min subsequent of treatment with 50 nM PMA in HL60 cells and primary monocytes/macrophages (one representative experiment is shown). CB_2 receptors stain as double band (60 kDa), PCNA (32 kDa) was used as loading control. When semi-quantified by densitometry no difference between treated vs. vehicle control over time was found.

phages. In an analogous experiment, we monitored CB_1 receptor trafficking in PBMCs on H_2O_2, PAO, and PMA challenge. As shown in Fig. 7E, H_2O_2 did not induce CB_1 receptor internalization in monocytes/macrophages but a pronounced externalization of CB_1 receptors in lymphocytes in response to H_2O_2 (263%) and PAO (310%) treatment. These data suggest that CB_1 receptor surface expression might be regulated via the same mechanism in immune cells.

3.5. Lymphocyte activation induces CB_2 receptor externalization and changes the trafficking response to the tyrosine phosphatase inhibitor PAO and PMA

Activation of CD4$^+$ lymphocytes with CD3/CD28 antibodies has been reported to result in CB_2 receptor externalization [58]. In order to assess the differential regulation of CB_2 receptor trafficking between activated and resting lymphocytes, cells were activated with CD3/CD28 overnight and compared with freshly thawed non-activated lymphocytes in terms of possible changes in receptor cell surface expression and the subsequent response to PAO and PMA treatment. In agreement with the preceding results, lymphocytes significantly externalized CB_2 receptors after activation (Fig. 8). Whereas PAO significantly externalized CB_2 receptors in resting lymphocytes (204%), PAO only showed a non-significant trend toward CB_2 receptor externalization in the activated population (131%). Notably, in activated lymphocytes, PMA reversed CD3/CD28 induced CB_2 receptor externalization, restoring surface expression levels equal to non-activated cells.

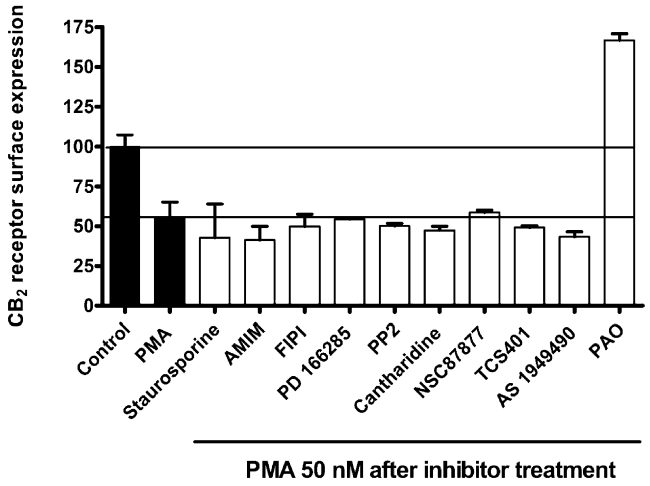

Fig. 6. Inhibition of distinct kinases and phosphatases to identify targets involved in PMA-induced CB_2 receptor internalization. $CD14^+$ monocytes/macrophages (1×10^6) were pre-incubated with various inhibitors and subsequently treated with 50 nM PMA for 30 min prior to FACS analysis. Inhibitor panel: Staurosporin (unselective protein kinase C; PKC); AMIM (anilino-monoindolylmaleimide; protein kinase C β2 inhibitor); FIPI (5-fluoro-2-indolyl des-chlorohalopemide; phospholipase D; PLD); PD 166285 (tyrosine kinases); PP2 (Src-family tyrosine kinases); Cantharidin (protein phosphatase 1 and 2A inhibitor); NSC 87877 (Src homology phosphatase 1 and 2; SHP-1, SHP-2); TCS 401 (protein-tyrosine phosphatase 1B inhibitor); AS 1949490: (SH2-containing 5′-inositol phosphatase inhibitor); PAO (phenylarsine oxide; protein tyrosine phosphatase inhibitor). Data show mean values ± SD, $N = 3$.

3.6. Lymphocyte donor differences in CB_2 receptor surface expression pattern

Lymphocytes generally displayed only low levels of CB_2 receptor at the cell surface (Fig. 9A). However, in a small number of donors (about one out of 10), a not further characterized subpopulation of lymphocytes with high CB_2 receptor surface expression levels (Fig. 9B, arrow) was observed, which we did not further characterize, but probably reflected a subpopulation of activated NK cells. In a typical experiment, PAO treatment-induced CB_2 receptor externalization in the lymphocyte fraction with low basal surface expression, resulting in an integrated externalization of CB_2 receptors for the whole lymphocyte population. In the rare donors with a high CB_2 receptor expression subpopulation PAO displayed a differential effect, externalizing CB_2 receptors in the low surface expressing cells and, in contrast, internalizing CB_2 receptors in cells with high basal surface expression (Fig. 9B). The resulting overall CB_2 receptor surface expression in the whole lymphocyte population was not significantly different from the control.

3.7. Clathrin and caveolin independence of PMA-induced endocytosis and possible involvement of lipid rafts in CB_2 receptor externalization

As we found CB_2 receptors in both cell membranes and lipid raft preparations from HL60 cells (Fig. 3B) and previous reports have suggested a caveolin- and/or clathrin-dependent internalization of CB_1 and CB_2 receptors, respectively [24,32,59,60], we further characterized the mechanism of CB_2 receptor internalization in primary immune cells by blocking these endocytotic pathways. PBMCs were incubated for 1 h with multiple inhibitors of clathrin- and caveolin-mediated endocytosis and subsequently treated with PMA to induce internalization (Fig. 10A). The established inhibitors of caveolin-mediated endocytosis methyl-β-cyclodextrine, a cholesterol-depleting agent [61–63], cantharidine, a serine/threonin phosphatase inhibitor [64] and PP2, a specific Src-kinase inhibitor [65], both involved in caveolin-mediated endocytosis, did not prevent PMA-induced endocytosis, thus suggesting a caveolin-independent endocytotic pathway. To assess the possible role of a clathrin-mediated endocytosis, cells were pre-incubated with two inhibitors of clathrin-mediated endocytosis. Amantadine, which stabilizes clathrin coated pits at the cell membrane [66], and dansylcadaverine, a potent inhibitor of clathrin-mediated endocytosis which acts by preventing clathrin polymerization [67], did not block PMA-induced internalization (Fig. 10B). These data suggest that CB_2 receptor internalization in PBMCs is mediated by caveolin and clathrin-independent endocytotic pathways, although this may be different in cells transfected with CB_2 receptor constructs. Interestingly, when MCF7 cells stably expressing CB_2GFP (Fig. 10C) and normal MCF7 cells with low CB_2 receptor surface expression were incubated with 500 nM of MCD or 1 μM of amphothericin B, which at this concentration also depletes cholesterol [68], a significant increase in CB_2 receptor surface expression was observed in both normal and CB_2 receptor transfected MCF cells (Fig. 10D and E). A similar increase in CB_2 receptor surface expression upon MCD treatment was also seen with other cell lines (not shown). This suggests that specific lipid membrane compartments may be involved in the basal internalization of these receptors or, alternatively, that the membrane architecture is artificially modified by MCD and amphotericin B, thus leading to an artificial recruiting of CB_2 receptors to the surface.

3.8. Localization of the intracellular CB_2 receptor pool

In order to identify the intracellular compartments in which the internalized CB_2 receptor pool resides, NIH3T3 mouse fibroblasts stably transfected with N-terminally eGFP-tagged murine CB_2 receptor (CB_2-GFP) were stained with specific markers for endoplasmatic reticulum (ER), lysosomes, early endosomes and mitochondria (Fig. 11). We also transfected other cell lines, including MCF7 cells, but NIH3T3 cells showed the strongest expression. Most cells showed a pronounced CB_2-GFP receptor expression in the perinuclear region, which however did not co-localize with the ER (Fig. 11, Panel A), the lysosomes (Fig. 11, Panel B) or mitochondria (Fig. 11, Panel D). According to these results, intracellular CB_2 receptors in NIH3T3 cells (and probably other cells) reside in as yet unidentified cytoplasmic compartments from where they may be recruited to the cell membrane.

3.9. pH mediated CB_2 receptor internalization

Because a lowered pH in the 6.5 range has been reported in both inflamed tissue and the microenvironment of growing tumors [69,70], we also studied the impact of pH alterations on CB_2 receptor surface expression in peripheral immune cells. After PBMCs had been exposed to pH-adjusted media for 2 h, CB_2 receptor surface levels were quantified. As shown in Fig. 12, pH 6.5 led to a partial internalization of CB_2 receptors in lymphocytes (~75% of pH 7.5 control). On the contrary, monocytes/macrophages were more sensitive toward higher pH as indicated by the significant internalization at pH 8.5. To further investigate the interplay of an altered pH and reactive oxygen species, the TPI H_2O_2 was added to cells after 1 h of pre-incubation at pH 6.5. Interestingly, rescue from the pH-mediated internalization phenotype and even a significant externalization (~150%) was observed in lymphocytes. In monocytes/macrophages H_2O_2 again counterbalanced the pH effect, showing the differential action of H_2O_2 and again reflecting the distinct localizations of CB_2 receptors in monocytes and lymphocytes (see above).

3.10. Impact of glucose metabolism on CB_2 receptor cell surface expression

Recently, mitochondria in peripheral cells and neurons have been suggested to contain functional CB_1 receptors [13,71].

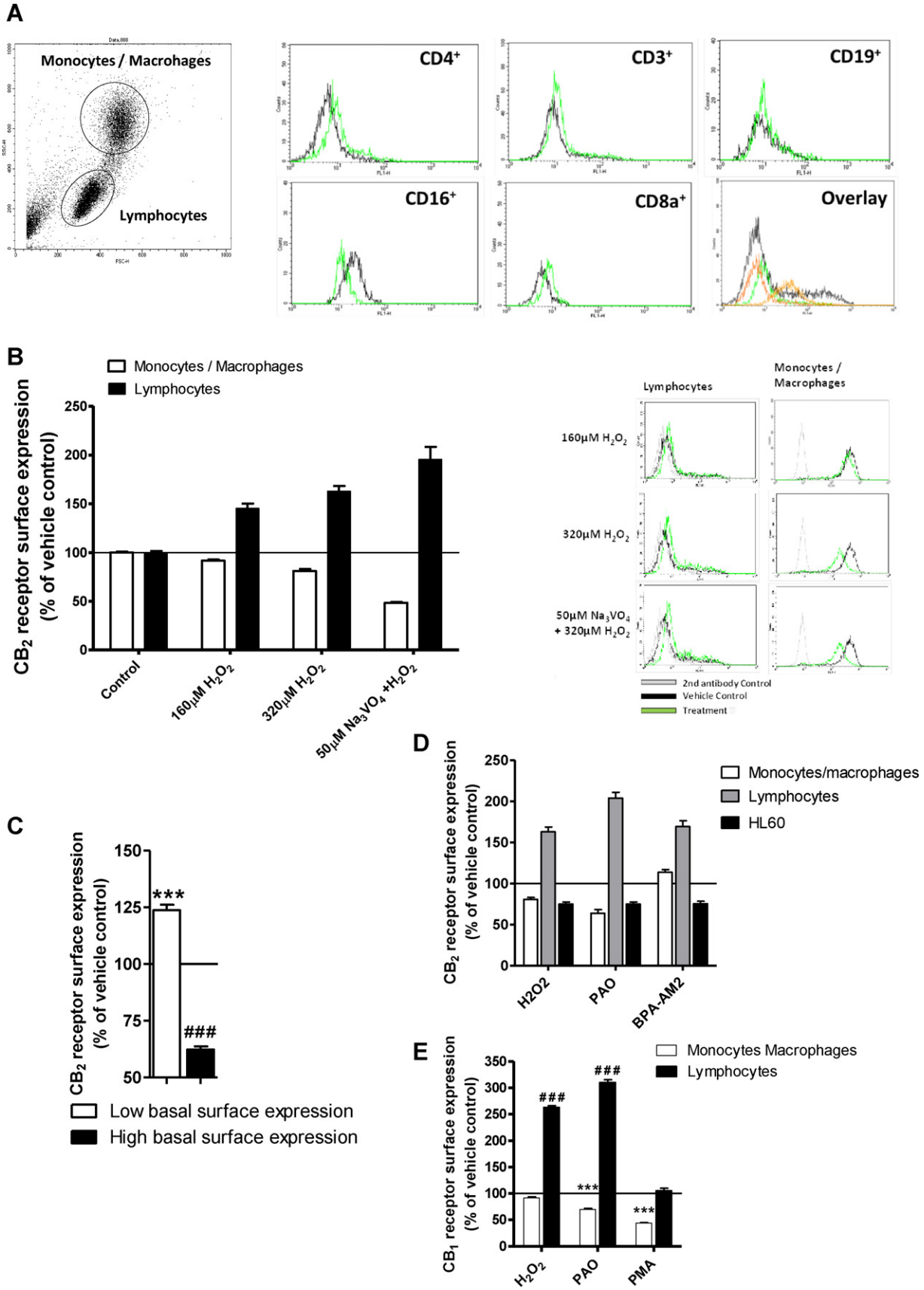

Fig. 7. CB_2 receptor surface expression is subject to a binary switch regulated by protein tyrosine phosphatases. (A) PBMCs isolated from buffy coat were gated into subpopulations of lymphocytes and monocytes/macrophages according to forward and side scatter profiles by analytical FACS for quantification of CB_2 receptor surface expression levels. Isolated lymphocytes (1×10^6) were incubated 1 h with the protein tyrosine phosphatase inhibitor PAO (5 µM), stained for CB_2 receptors and subgated for $CD3^+$, $CD4^+$, $CD16^+$ and $CD19^+$ subpopulations for analytical FACS. Overlay depicting differential basal CB_2 receptor surface expression of $CD3^+$ (green), $CD4^+$ (red) and $CD16^+$ (orange) T cell subpopulations compared to whole lymphocyte population (black). Shown are representative graphs of independent experiments. (B) Human primary $CD14^+$

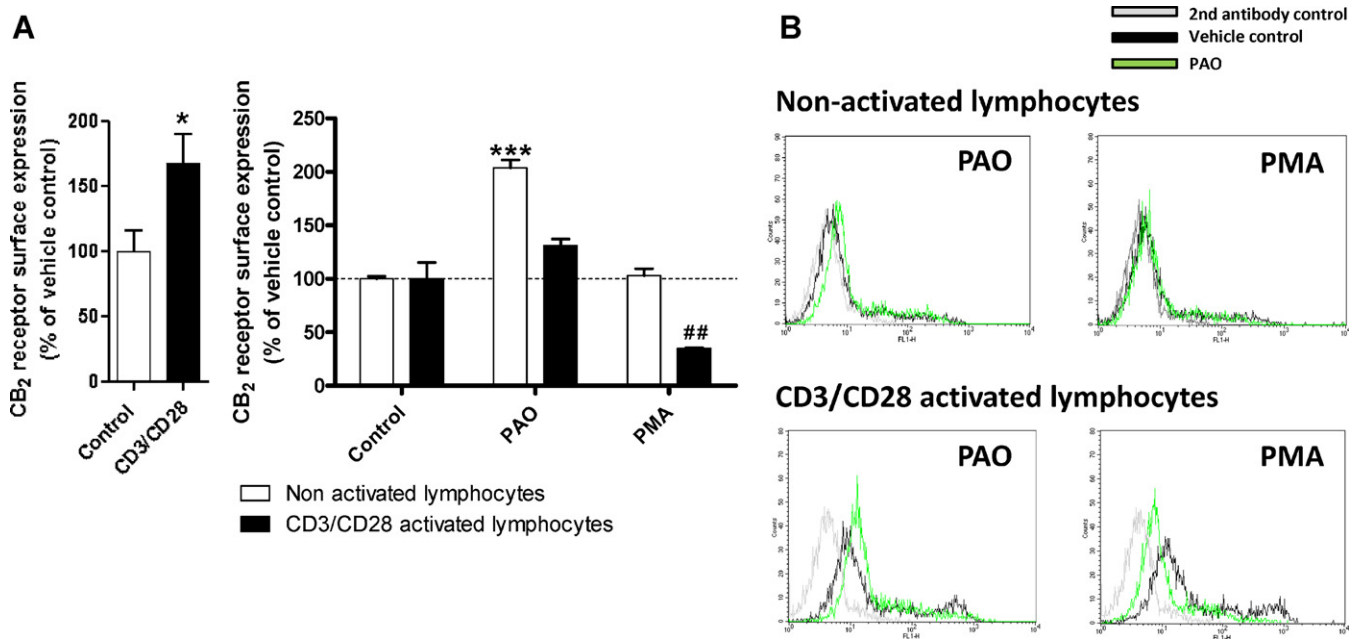

Fig. 8. Effect of lymphocyte activation on CB_2 receptor trafficking. 1×10^6 lymphocytes were activated over night with CD3/CD28 for 18 h and subsequently treated with 5 μM PAO for 1 h or 50 nM PMA for 30 min (activated lymphocytes) or treated immediately after thawing (resting lymphocytes). Nonspecific binding of Abs to Fc receptors was negligible. At least 5×10^3 gated cells were quantified in analytical FACS experiments. Data show mean values ± SEM, $N = 6$, of two donors from two independent experiments. Cells were analyzed with Student's t-test, $^{*}p < 0.05$, or two-way ANOVA followed by Tukey post hoc analysis $^{***}p_{adj.} < 0.001$, $^{\#\#}p_{adj.} < 0.01$.

Elevated lactate levels have been reported in wound healing [72] where CB_2 receptors are likely to be expressed, and lactate is secreted in high amounts as a metabolite of anaerobic glucose metabolism by growing malignant cells [73,74], a mechanism called the Warburg effect. Although in our experiments we could not detect CB_2 receptors in mitochondria (Fig. 11), we nonetheless wanted to investigate the potential metabolic link to CB_2 receptor trafficking. To assess the putative effect of glucose metabolism and elevated lactate in the medium on CB_2 receptor surface expression, HL60 cells were incubated in an initial experiment with media containing different concentrations of glucose and ammonium-lactate as alternative energy source in glucose reduced (1 mg/ml) or glucose-free medium as adapted from Stern et al. [72]. Medium supplemented with ammonium lactate-induced a maximal internalization of CB_2 receptors (supplemental Fig. 2A), but also resulted in a pH shift of the medium to pH 8.7. Thus, in a next set of experiments ammonium-lactate was substituted by sodium-lactate, which is pH neutral (supplemental Fig. 2B), showing no significant effect on CB_2 receptor surface expression and thereby indicating that the pH shift (see also above) rather than the lactate ion-induced receptor internalization. U937 cells differentiated into macrophages express higher levels of CB receptors than undifferentiated U937 cells (data not shown) and activated macrophages are reported to show anaerobic glycosylation [75]. To investigate the possibility that anaerobic glycosylation modulates CB receptor surface expression, macrophages derived from PMA-stimulated U937 cells were shifted from anaerobic glycolysis to oxidative phosphorylation through incubation with dichloroacetate (DCA) alone or DCA combined with 2-deoxyglucose (2-DG) and lactate as an alternative substrate for oxidative phosphorylation in the mitochondria. DCA shifts cells from anaerobic to aerobic glycolysis by inhibition of pyruvate dehydrogenase (PDK), a negative regulator of oxidative phosphorylation [76], whereas 2-DG is an inhibitor of glycolysis at the hexokinase level. As shown in supplemental Fig. 2, both treatments resulted in a trend toward reduction of CB_2 receptor surface expression. In order to test if the dramatic differences in CB receptor surface expression between HL60 cells and one aberrant HL60 clone lacking CB receptor surface expression [50] could be explained by differences in glucose metabolism by these cells, cells were incubated with DCA or oxamate, an inhibitor of glycolysis which blocks conversion of lactate into pyruvate and vice versa. As shown in supplemental Fig. 2, oxamate-induced a significant but small externalization of CB_2 receptors in the HL60 negative cell line, indicating sensitivity of the internalized CB_2 receptor pool to glucose metabolism. However, because the effects were less dramatic than those obtained with the TPIs they are likely to be indirect and therefore are not a trigger of the binary biochemical switch (see above).

4. Discussion

In this study we challenge the widely accepted view that agonist stimulation leads to CB receptor internalization (i.e. trafficking) in primary peripheral cells. We show that CB_2 receptor trafficking is mediated by ligand-independent mechanisms in immune cells and different cell lines. So far, the majority of studies has focused on CB_1 receptor transfected cells and neuronal cells [23,25,31,32]. The internalization of CB_1 receptors in response to

monocytes/macrophages and lymphocytes treated with protein tyrosine phosphatase inhibitors for 1 h at indicated concentrations. Hydrogen peroxide (H_2O_2); sodium orthovanadate (Na_3VO_4). (C) Two HL60 clones differing in basal CB_2 receptor surface expression (for FACS characterization see Fig. 4A), treated for 1 h with 320 μM H_2O_2. (D) Effect of three different TPIs on CB_2 receptor surface expression in peripheral immune cells. Cells were treated for 1 h with 320 μM H_2O_2, 5 μM PAO and 100 μM benzylphosphonic acid bis-acetoxymethyl ester (BPA-AM_2). (E) Effects of TPIs PAO (5 μM), H_2O_2 (320 μM) and PMA (50 nM) on CB_1 receptor surface expression. Data show mean values ± SEM, $N = 9$ from 3 different donors and 3 independent experiments. Nonspecific binding of Abs to Fc receptors was negligible. At least 5×10^3 gated cells were quantified in analytical FACS experiments. Effects were analyzed by one-way ANOVA followed by post hoc test for linear trend, indicating $p < 0.001$ for monocytes/macrophages and lymphocytes. (C–E) were analyzed with Student's t-test, $^{***/\#\#\#}p < 0.001$. (For interpretation of the references to color in this figure legend, the reader is referred to the web version of the article.)

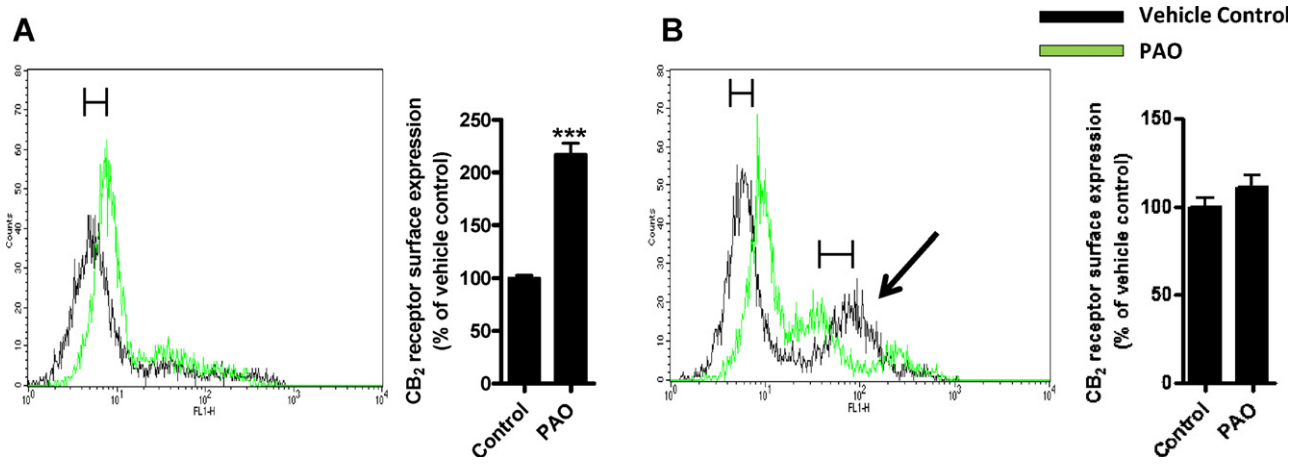

Fig. 9. CB_2 receptor trafficking in lymphocytes in response to PTP inhibition is donor dependent. (A) Lymphocyte population representing the normal CB_2 receptor expression pattern observed in the majority of all donors. (B) In rare cases, donors displayed a population of lymphocytes with high CB_2 receptor surface expression (arrow). When stimulated with 5 μM PAO for 1 h, subpopulations with high CB_2 receptor surface expression internalized CB_2, receptors in these population but externalized CB_2 receptors in the low CB_2 receptor expressing population. Nonspecific binding of Abs to Fc receptors was negligible. Data show mean values ± SD from 3 independent experiments and analyzed with unpaired *t*-test, $^{***}p < 0.005$. At least 5×10^3 gated cells were quantified in analytical FACS experiments.

agonist stimulation via both clathrin-coated-pits and the caveolae pathway has been described for both heterologous expression systems [77] and primary neurons [78–80]. That functional cell surface receptors are internalized by endocytosis upon activation is a fundamental component of GPCR biology [81] as a controlled internalization of receptors from the cell surface modulates cell sensitivity to specific ligands. It was shown that CB_1 receptors do not recycle following constitutive or agonist-induced internalization but instead exhibit a primarily degradative phenotype [25]. In contrast to the recycling hypothesis, downregulation of CB_1 receptors following chronic agonist stimulation has been widely reported [82], and GASP-1 [80,83] and AP3 [84], adaptor proteins associated with sorting and delivery of receptors to lysosomes, were demonstrated to interact with CB_1 receptors. On the other hand, very limited data is available on cellular CB_2 receptor localization and trafficking mechanisms in primary cells [17,31]. Although it has been suggested that CB_2 receptors internalize via Rab5-mediated endocytosis and that internalized receptors are recycled via a Rab11-associated pathway upon agonist stimulation [31], these studies have been carried out in overexpression systems. While in our study we confirm that CB_2 receptors recombinantly expressed in CHOK1 cells internalize upon agonist stimulation (Fig. 1), we also provide evidence that agonist stimulation of human primary monocytes/macrophages and lymphocytes, as well as HL60 and MCF7 cells does not lead to internalization of cell-surface CB_2 receptors (Fig. 1). Because a rapid phosphorylation of CB_2 receptors upon CP55,940 stimulation in HL60 cells was shown [27] we conclude that the lack of internalization is not due to the absence of receptor phosphorylation in these cells. Interestingly, different agonists may also mediate different effects on receptor trafficking [32], thus exhibiting a similar functional heterogeneity reported for CB_2 receptor inverse agonists [85]. Although CP55,940 robustly internalizes receptors in cells heterologously expressing CB_2 [32], in our hands, this agonist did not trigger CB_2 receptor trafficking in primary cells. Thus, observations obtained in heterologous expression systems may not exactly reflect the trafficking behavior in peripheral cells such as immune cells and need to be interpreted cautiously. Differences in trafficking behavior might be due to cell type specific expressions of proteins involved in the endocytotic machinery, divergent post-translational modification or distinct protein–protein interaction patterns [86]. The importance of CB receptor surface expression changes in disease may be related to such mechanisms, in addition to gene expression [22]. In our hands, different cell lines showed significant differences between CB receptor gene expression and receptor cell-surface expression (Figs. 1 and 2). In many cell types, CB receptors in the cell membrane are lacking despite the presence of CB receptors in cytoplasmic compartments (i.e., positive in Western blots but negative in FACS experiments). Moreover, clones from the same cell line may exhibit dynamic changes in CB receptor surface expression (Figs. 2 and 3). Such observations indicate the necessity to perform experiments in primary cells to allow the results to be contextualized within more physiological settings.

Importantly, GPCR surface expression not only regulates accessibility of receptors to ligands but determines signaling from distinct compartments. The view of exclusive GPCR cell surface expression after synthesis has recently been challenged for CB_1 receptors by independent reports showing that endogenously expressed CB_1 receptors in adipocytes and neurons are localized and functional in intracellular compartments [87–89], with one report indicating that only about 15% of CB_1 receptors are surface expressed [90]. Elegant studies by Brailoiu et al. [91] and Benard et al. [71] have demonstrated signaling of intracellular CB_1 receptors located in lysosomes and mitochondria, respectively, suggesting that the intracellular pool of receptors is functional. The latter study shows significant functional signaling of mitochondrial CB_1 receptors in neurons and thus opens up an entirely new field of research [71]. The impact of intracellular CB receptor signaling on cell physiology remains to be established but is likely to be of relevance upon ligand treatment, as many compounds targeting CB receptors are lipophilic and readily cross cell membranes.

While mitochondria, lysosomes, endosomes and the perinuclear region have already been suggested as intracellular compartments of storage, redistribution and degradation for CB_1 receptors [23,25,84,92], little is known about intracellular CB_2 receptors. We observed pronounced perinuclear localization of tagged overexpressed CB_2 receptor constructs in several cell lines with only partial membrane localization of the receptor (data not shown). NIH3T3 cells expressing a CB_2 receptor construct N-terminally tagged with eGFP (CB_2-GFP) showed no specific staining of endoplasmatic reticulum, lysosomes and mitochondria, indicating that CB_2-GFP does not co-localize with these compartments. Some yellow areas in the merged picture of the early endosome

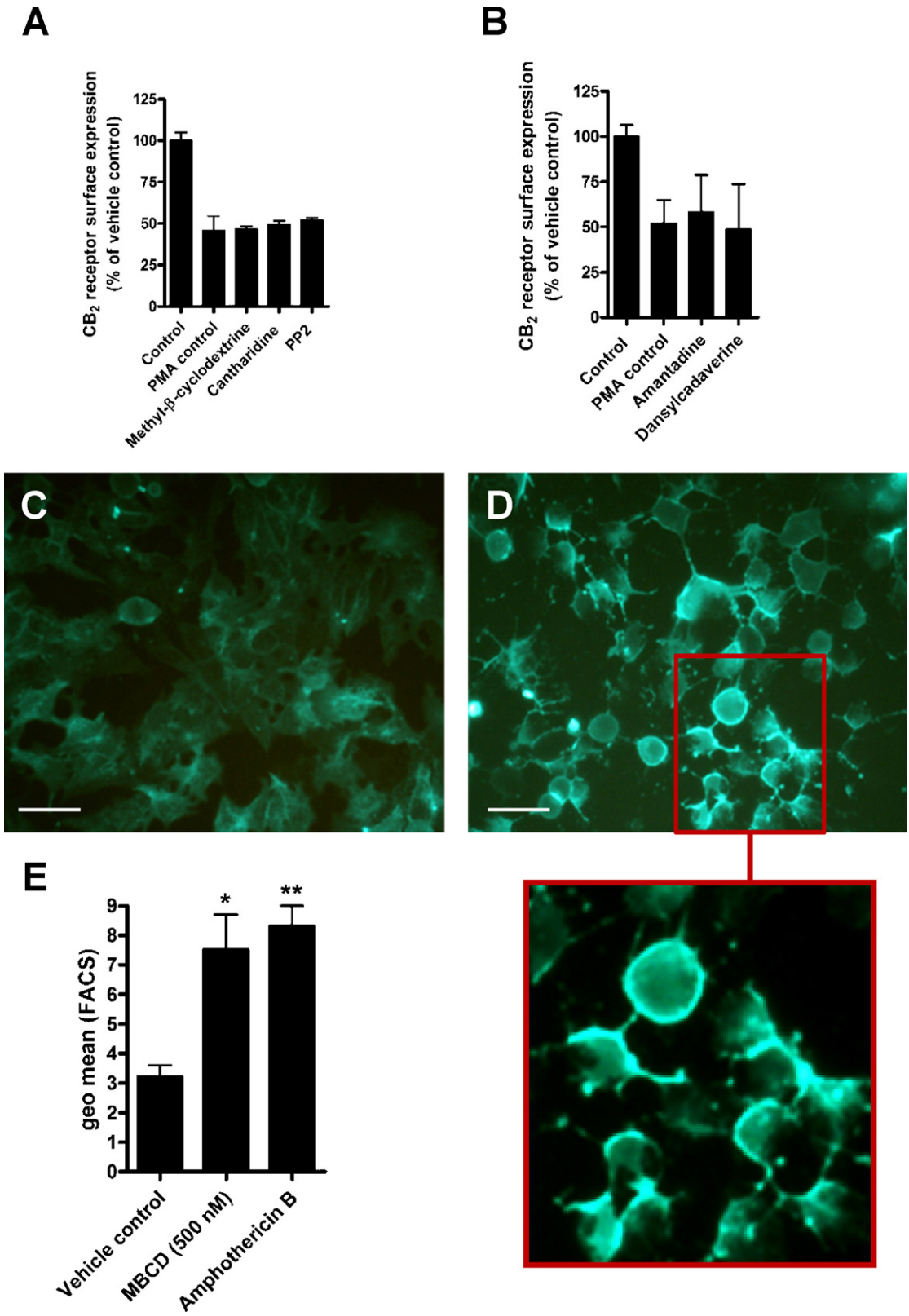

Fig. 10. PMA-induced CB_2 receptor internalization is mediated by an apparently clathrin- and caveolin-independent process in primary monocytes/macrophages. (A) 1×10^6 cells were pre-incubated for 1 h with different inhibitors of caveolin-mediated endocytosis or (B) clathrin-mediated endocytosis followed by addition of PMA to elicit receptor internalization. Inhibitors were used at the following concentrations: Methyl-β-cyclodextrine (2.5 mM), cantharidine (5 μM), PP2 (20 μM), amantadine (100 μM), dansylcadaverine (100 μM). (C) CB_2-GFP receptor transfected MCF7 cells show significant cytoplasmic expression. (D) MBCD (500 nM) treatment for 30 min led to increased CB_2 receptor localization in cell membranes. (E) In nontransfected MCF7 cells treatment with MBCD (500 nM) and amphothericin B (1 μM) for 3 h showed a significant increase of CB_2 receptor surface expression. Mean values ± SD are shown, $N = 3$. Data was analyzed with paired t-test, $^*p < 0.05$; $^{**}p < 0.01$.

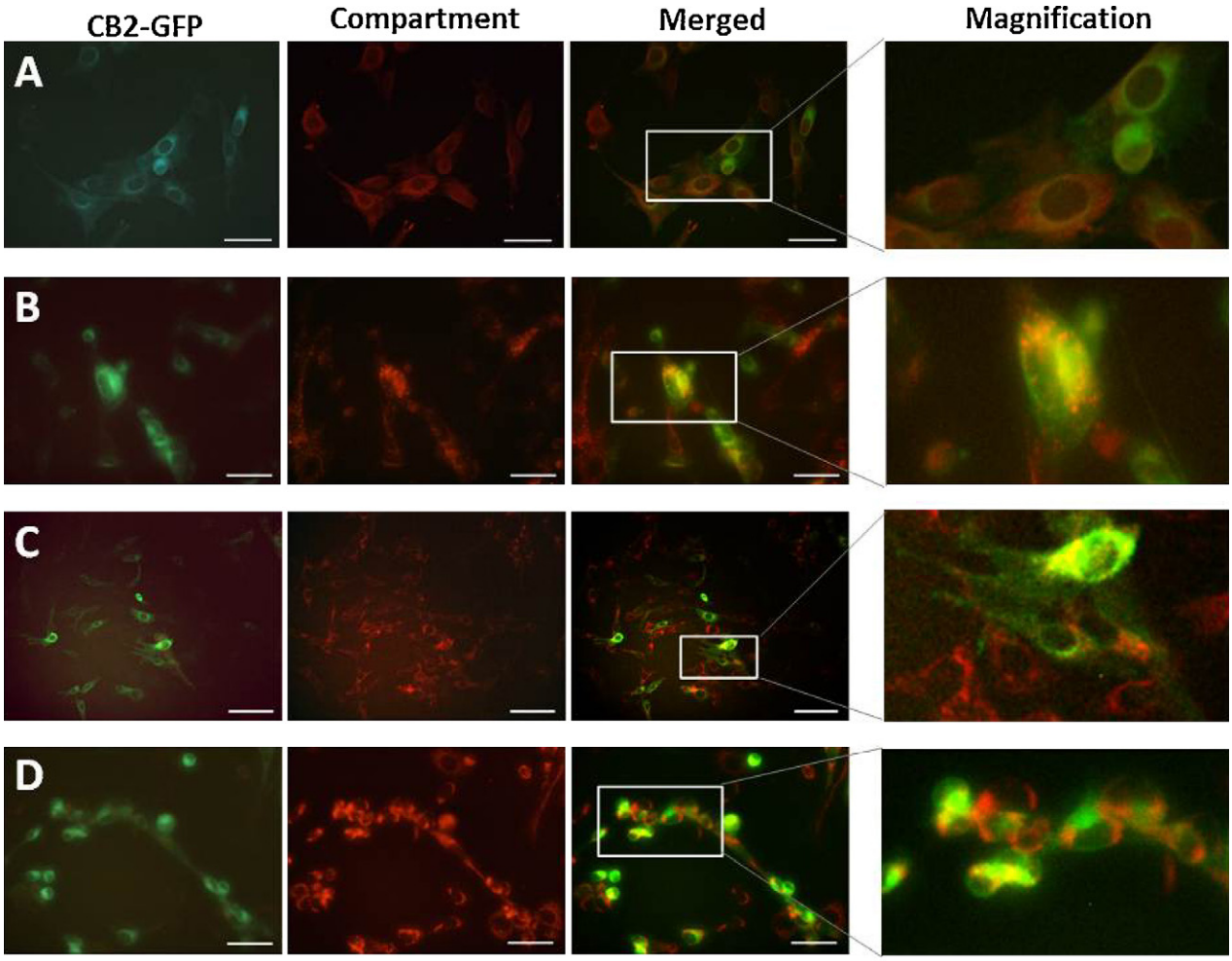

Fig. 11. Localization of intracellular CB_2-GFP in NIH3T3 mouse fibroblasts. Logarithmically growing NIH3T3 cells stably expressing the receptor with an N-terminal eGFP tag were stained with different markers of intracellular compartments as described in the experimental procedures. (A) Endoplasmatic reticulum immunostained with PDI Ab, SPA-891 (Stressgen). (B) Lysosomes stained with Lysotracker® (Invitrogen). (C) Early endosomes immunostained with early endosome antigen 1 (EEA1). (D) Mitochondria stained with Mitotracker® (Invitrogen). The scale bar is 50 μm. Representative pictures from independent experiments are shown.

stain suggested putative co-localization of CB_2 receptors with endosomes (Fig. 11), which is likely due to overexpression of CB_2-GFP in this cell as in preparations with lower expression levels endosome stain and GFP signal do not co-localize.

To further characterize the endocytotic pathways involved in CB_2 receptor internalization, we investigated caveolin and clathrin-mediated endocytosis in primary monocytes/macrophages. Both pathways have been described to be involved in CB_1 and CB_2 receptor internalization within the context of heterologous expression cells (both receptors) and in endogenously expressing cells (CB_1) [24,77,80]. Pathway specific inhibitors did not reduce PMA-induced CB_2 receptor endocytosis, suggesting caveolin- and clathrin-independent internalization pathways in primary monocytes/macrophages.

Accumulating evidence from a number of studies indicate that homo- and heterodimerization of GPCRs is a common phenomenon [93]. For example, CB_1 receptors were shown to form heterodimers with the D2 dopamine receptor, the μ-, κ- and δ-opioid receptor, the orexin-1 receptor, the $A2_A$ adenosine receptor and the β_2-AR receptor [94–97]. Additionally, using an anti-CB_1 receptor antibody, which preferentially recognizes the multimeric form of the receptor, homodimerization and oligomerization of CB_1 receptors has been shown by SDS-Page [51] and in immunohistochemical studies [51,98,99]. HL60 cells endogenously express high levels of CB receptors (similar to primary monocytes/macrophages) and surface expression levels appears to be dynamic in this cell line and do vary significantly even between certified batches of original suppliers such as ATCC and DSMZ (Fig. 3). Notably, the CB_1 and CB_2 receptor surface expression ratio stayed at a constant level of 1:1, independently of absolute expression levels. This led us to hypothesize the potential heterodimerization of CB_1 and CB_2 receptors in this cell line. Typically, in immunoprecipitation studies two receptors with distinct epitope tags are heterologously expressed in cell lines, allowing for subsequent precipitation. However, artificially high levels of protein expression and alteration of protein structure due to introduction of tags creates the possibility of detecting false positives in these systems. For the first time we provide evidence for the formation of heterocomplexes of CB_1 and CB_2 receptors in untransfected HL60 cells, utilizing different antibodies for each receptor. In order to establish a second line of evidence for heterodimerization, we created a shRNA partial CNR1 knock down HL60 mutant, which showed 60% reduction of CB_1 receptor surface expression compared to the mock transfected control. Notably, this reduction of CB_1 receptor surface expression was accompanied by a stoichometrically matching 54% decrease in CB_2 receptor surface expression (Fig. 4D), indicating that heterocomplex formation may be a prerequisite for CB_1 and CB_2 receptor externalization in this cell line. Altered receptor signaling has been reported to be a functional consequence of GPCR heterodimer formation and some of the many discrepancies observed in CB

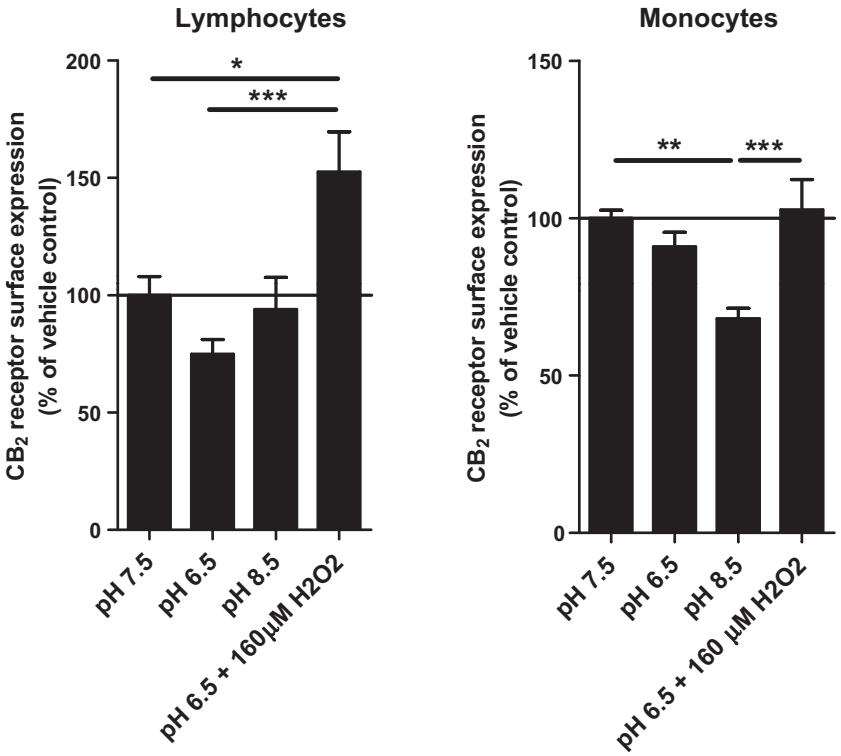

Fig. 12. pH-dependent internalization of CB_2 receptors in primary $CD14^+$ lymphocytes and monocytes/macrophages. 1×10^6 cells were incubated in low glucose medium (1 mg/ml) at pH 6.5, 7.5 and 8.5 for 2 h. In treatments with hydrogen peroxide, 160 μM H_2O_2 was added after 1 h pre-incubation in pH 6.5 medium and co-incubated for 1 h after addition. At least 5×10^3 gated cells were quantified in analytical FACS experiments. Data show mean values ± SD, $N = 3$ and were analyzed by one-way ANOVA followed by post hoc Tukey test, $^{**}p_{adj.} < 0.01$, $^{***}p_{adj.} < 0.001$.

receptor signaling between different cell types could be due to CB_1/CB_2 receptor heterodimerization. It will be interesting to study the role of CB receptor heterodimerziation in promyelocytic cells and the potential association to other cannabinoid-sensitive GPCRs like GPR55 [100].

CB_2 receptors are expressed in all major leukocyte subsets in human blood [17] with surface expression levels varying from almost absent to very pronounced (Figs. 8 and 9). Many of the studies reporting the role of CB receptors in immune regulation have utilized SDS-Page Western blots of whole cell extract or RT-PCR to demonstrate the presence of CB receptors in particular cells [101,102]. A limitation of these approaches is that although total expression levels are quantified no information on cell surface expression of the protein is obtained. Regulation of GPCR cell surface expression is a commonly noted phenomenon [103]. Data obtained in our study indicate low, high and dynamically fluctuating CB_2 receptor surface expression patterns in diverse cell lines. Based on these observations, we were interested to identify mechanisms involved in the modulation of CB_2 receptor surface expression in immune cells. PMA only triggered internalization of CB receptors expressed at the surface but in none of the experiments did it externalize CB receptors. Since PMA has multiple effects, several of which are independent of PKC [104], it is difficult to speculate on the underlying mechanism. TPIs like PAO can trigger both internalization and externalization of CB receptors, depending on the basal state of cellular receptor localization before treatment.

In this study we demonstrate that TPIs elicit robust cell-type specific CB_2 receptor trafficking in peripheral mononuclear cells and trigger a binary biochemical switch. Quantification of surface expression by analytical FACS shows, in agreement with previous studies [17], that monocytes/macrophages are among the cells with the highest CB_2 receptor surface expression, whereas resting lymphocytes do display the lowest levels of blood-derived leukocytes [17,58]. Treatment of PBMCs with increasing concentrations of H_2O_2, a reversible TPI, and pervanadate, an irreversible TPI, resulted in a concentration-dependent trafficking response. Monocytes/macrophages with high basal surface expression internalized CB_2 receptors, whereas a pronounced externalization of CB_2 receptors in lymphocyte subsets was observed. At a mechanistic level, internalization and externalization of GPCRs is mediated by protein–protein interactions and our data suggest that it is only partially dependent on lipid rafts, but very strongly on tyrosine phosphorylation. Since we observe full internalization or full externalization upon incubation with TPIs, we termed this mechanism "binary switch". The PTP inhibitor phenylarsine oxide was most effective in triggering this biochemical switch and is therefore a novel tool agent to study the amount of intracellular receptors that can be recruited to the cell surface. Treatment with PAO for 30 min prior to FACS analysis provides an excellent means to distinguish between CB receptor de novo expression and trafficking.

H_2O_2 is an endogenously produced reversible TPI and its transient release with other reactive oxygen species (ROS) by phagocytic leukocytes during the immune response is well documented. Apart from its microbe-killing properties accumulating evidence suggests important second messenger functions for H_2O_2 in T cell activation and leukocyte migration [105]. The action of endogenously produced H_2O_2 is very locally restricted, due to enzymatic removal by catalase, glutathione peroxidase and peroxiredoxins [106]. These scavenger enzymes are distributed throughout the cell, with catalase displaying one of the fastest enzymatic kinetics (4 million molecules/s), resulting in a 1 ms half-life for H_2O_2 and an estimated effector range of a few molecular diameters [106]. Thus, a very local regulation of PTP activity within the cell, close to the production site of H_2O_2 has been proposed.

This also explains the need and validity for the addition of micromolar to low millimolar doses of exogenous H_2O_2 to simulate endogenous H_2O_2 production, which is estimated to be in the low nanomolar range in steady-state cells [107], but reaching μM levels at sites of inflammation [36,108]. In contrast to the other ROS species such as superoxide anion and hydroxyl radicals, H_2O_2 is a rather mild oxidant that targets primarily the essential cysteine residues of PTPs with a low pK_a of 4.7 to 5.4 in their conserved catalytic center, whereas only few other proteins are oxidized [109] due to a prevalent pK_a of ~8.5 of most sulfhydryl groups of cysteine residues [110]. Oxidation of the catalytic center renders PTPs completely inactive, thereby resulting in a shift toward protein phosphorylation.

We studied lymphocyte subpopulations after incubation with PAO. A general pattern of CB_2 receptor externalization was observed in $CD4^+$, $CD3^+$ and $CD8a^+$ T-cells with the exception of $CD16^+$ natural killer (NK) cells, which displayed internalization. Comparing basal surface expression of NK cells with the other subtypes, it is evident that NK cells show the highest basal CB_2 receptor cell surface expression of all T cells, in agreement with previous reports [17]. Therefore, the proposed pattern of binary trafficking behavior is also reflected within the lymphocyte population. The next set of experiments was designed to rule out that unspecific side effects of the PTP inhibitors were responsible for the changes in surface expression. HL60 cells, a widely used promyelocytic leukemia cell line, has the potential to differentiate into a granulocytic, macrophage or neutrophil phenotype. Different batches of these cells from ATCC and DMSZ, although certified, differed markedly in basal CB_1 and CB_2 receptor expression. Consistent with the binary switch hypothesis, incubation of cells with H_2O_2-induced both externalization and internalization of receptor according to basal expression levels, thereby demonstrating that even within one model system both trafficking directions are regulated by a "tyrosine phosphorylation tone". In an additional experiment, PBMCs and HL60 cells were incubated with 3 different PTP inhibitors, reflecting the predicted trafficking pattern in all combinations with a single exception of BPA-AM_2 in monocytes, leading to a slight externalization. Finally, we also showed CB_1 receptor internalization in monocytes/macrophages and CB_1 receptor externalization in lymphocytes, on incubation with H_2O_2 and PAO, mirroring the pattern of CB_2 receptor trafficking. The immediate upregulation of CB_1 and CB_2 receptors within 1 h of compound incubation indicates the mobilization of intracellular pools rather than de novo synthesis of receptors. This hypothesis is also supported by the lack of receptor degradation upon internalization and the fact that previous reports have described lymphocytes to be CB_1 and CB_2 receptor positive in SDS-PAGE and PCR [49,111], despite lacking surface expression as indicated by FACS analyses. Since PAO triggers the switch in both directions (i.e. binary), it is unlikely that these events are GRK-mediated phosphorylations of the receptor [24].

To better appreciate the importance of protein PTP activity for tyrosine phosphorylation levels one has to keep in mind that protein PTPs are powerful negative regulators compared to the phosphorylation activity of protein tyrosine kinases (PTKs). Dephosphorylation by PTPs is a first order reaction, whereas phosphorylation by PTKs requires ATP and therefore is a second order reaction. This results in a 100–1000-fold higher turnover rate of an active PTP compared to a PTK [109]. Due to the consistent observations of robust CB_2 receptor trafficking in response to distinct unspecific PTP inhibitors we were interested in identifying the relevant target PTPs by employing specific inhibitors. PTPs have received much less attention compared to PTKs and the function of most PTPs expressed in immune cells is still far from clear [112]. Several PTPs have been reported to be expressed at high levels exclusively in cells of hematopoietic origin or to play a role in T cell activation, a process known to stimulate CB_2 receptor externalization [58]. Notably, it is known that PTPs are non-redundant, display a striking degree of specificity and are not promiscuous house-keeping enzymes [113], additionally illustrated by the fact that the number of genes for PTKs (107) and PTPs (90) are very similar, with at least 45 different PTPs expressed in T cells [112]. Inhibition of several putative target PTPs, including CD45, an important tyrosine phosphatase in leukocytes, SHP-1, SHP-2, HePTP and PTP1B did not affect CB_2 receptor cell surface expression, rendering the search for the target PTP(s) unresolved.

Lymphocyte CB_2 surface expression has been reported to be very low in resting cells [17,58], consistent with the results of this study. The externalization of CB_2 receptors upon activation of T cells has been reported previously [58], suggesting dynamic regulation of CB receptor signaling under inflammatory conditions. We were therefore interested in the impact of PTP inhibition and PMA on activated lymphocytes. CD3/CD28 activated lymphocytes displayed higher surface expression than resting lymphocytes, in agreement with results from a previous report [19]. Notably, significant PAO-induced CB_2 receptor externalization was present only in resting lymphocytes, indicating that CD3/CD28 activation already depleted the available intracellular CB_2 receptor pool for further externalization. Interestingly, PMA reversed CD3/CD28-induced CB_2 receptor externalization, thereby restoring expression levels comparable to those of resting cells, whereas PMA had no significant effect on resting T cells with low surface expression levels. The normal CB_2 receptor surface expression pattern of lymphocytes from donors was characterized by a major population displaying very low surface levels and few cells with elevated surface levels. However, in a small number of donors (about 10%) a significant, but as yet uncharacterized subpopulation of lymphocytes with high CB_2 receptor surface levels was found. In these donors PAO-induced subpopulation specific CB_2 receptor internalization and externalization in accordance with the binary switch hypothesis, depending on basal surface expression levels prior to PAO stimulation.

Based on reports of lowered pH under inflammatory conditions and in the microenvironment of malignant tumors, we were interested in the effects of altered pH on CB_2 receptor surface expression in PBMCs, which are known to migrate and accumulate at these sites [114]. pH values as low as pH 6.5 have been reported [115] and both monocytes/macrophages and lymphocytes responded with CB_2 receptor internalization, with a more pronounced effect in lymphocytes (25% vs. 9% internalization). Elevated levels of reactive oxygen species are also hallmarks of inflammatory and tumor tissue, a condition we simulated by co-challenging cells with lowered pH and H_2O_2. H_2O_2 rescued the pH-mediated internalization, indicating interplay of the two parameters in physiological settings. We also assessed the impact of altered glucose metabolism reported for activated macrophages [75] on CB_2 receptor cell surface expression (supplemental Fig. 2), indicating glucose metabolism independency of CB_2 receptor surface expression in macrophages and HL60 cells.

In summary, our results show that agonist exposure does not result in CB_2 receptor internalization in important subsets of primary immune cells and several cell lines, contrasting with the data obtained so far from heterologous expression models. Additionally, we report on a binary biochemical switch of CB_2 receptor cell surface expression which is under the control of PTPs and regulates trafficking of CB_2 receptors from intracellular compartments to the cell membrane or internalization of CB_2 surface receptors, depending on the basal state of the receptor prior to treatment. Based on these data it is feasible that CB_2 receptor expression in primary cells is strongly and dynamically regulated by yet to be characterized trafficking mechanisms. For

the first time we provide experimental evidence for oligomerization and heterocomplex formation of CB_1 and CB_2 receptors in the cell membrane of HL60 cells endogenously expressing both receptors. Our findings may have a significant impact on further studies elucidating the therapeutic potential of CB_2 receptor-selective ligands, as receptor availability for ligand binding is a crucial determinant for drug action. Moreover, in order to develop therapeutic strategies targeting CB_2 receptors it is important to understand the regulation of trafficking (i.e. intracellular vs. extracellular receptors) under physiological and pathophysiological conditions.

Acknowledgments

This work was financed by the Swiss National Science Foundation research grant SNF_ 120672 and supported by the University of Bern Foundation and the Novartis Research Foundation grant 10B48.

Appendix A. Supplementary data

Supplementary data associated with this article can be found, in the online version, at doi:10.1016/j.bcp.2012.02.014.

References

[1] Howlett AC, Reggio PH, Childers SR, Hampson RE, Ulloa NM, Deutsch DG. Endocannabinoid tone versus constitutive activity of cannabinoid receptors. Br J Pharmacol 2011;163:1329–43.
[2] Yao B, Mackie K. Endocannabinoid receptor pharmacology. Curr Top Behav Neurosci 2009;1:37–63.
[3] Idris AI, Ralston SH. Cannabinoids and bone: friend or foe. Calcif Tissue Int 2010;87:285–97.
[4] Finn DP. Endocannabinoid-mediated modulation of stress responses: physiological and pathophysiological significance. Immunobiology 2010;215:629–46.
[5] Guindon J, Hohmann AG. The endocannabinoid system and pain. CNS Neurol Disord Drug Targets 2009;8:403–21.
[6] Karsak M, Gaffal E, Date R, Wang-Eckhardt L, Rehnelt J, Petrosino S, et al. Attenuation of allergic contact dermatitis through the endocannabinoid system. Science 2007;316:1494–7.
[7] Bab I, Zimmer A. Cannabinoid receptors and the regulation of bone mass. Br J Pharmacol 2008;153:182–8.
[8] Pacher P, Mechoulam R. Is lipid signaling through cannabinoid 2 receptors part of a protective system. Prog Lipid Res 2011;50:193–211.
[9] Oesch S, Gertsch J. Cannabinoid receptor ligands as potential anticancer agents—high hopes for new therapies. J Pharm Pharmacol 2009;61:839–53.
[10] Mackie K. Cannabinoid receptors: where they are and what they do. J Neuroendocrinol 2008;20(Suppl. 1):10–4.
[11] Klein TW, Newton C, Larsen K, Lu L, Perkins I, Nong L, et al. The cannabinoid system and immune modulation. J Leukoc Biol 2003;74:486–96.
[12] Galiegue S, Mary S, Marchand J, Dussossoy D, Carriere D, Carayon P, et al. Expression of central and peripheral cannabinoid receptors in human immune tissues and leukocyte subpopulations. Eur J Biochem 1995;232:54–61.
[13] Tedesco L, Valerio A, Cervino C, Cardile A, Pagano C, Vettor R, et al. Cannabinoid type 1 receptor blockade promotes mitochondrial biogenesis through endothelial nitric oxide synthase expression in white adipocytes. Diabetes 2008;57:2028–36.
[14] Larrinaga G, Begoña S, Itxaro P, Blanco L, Maria LC, Pinto FM, et al. Cannabinoid CB1 receptor is downregulated in clear cell renal cell carcinoma. J Histochem Cytochem 2010;58:1129–34.
[15] Leonti M, Casu L, Raduner S, Cottiglia F, Floris C, Altmann KH, et al. Falcarinol is a covalent cannabinoid CB1 receptor antagonist and induces pro-allergic effects in skin. Biochem Pharmacol 2010;79:1815–26.
[16] Onaivi ES, Ishiguro H, Gong J-P, Patel S, Perchuk A, Meozzi PA, et al. Discovery of the presence and functional expression of cannabinoid CB2 receptors in brain. Ann N Y Acad Sci 2006;1074:514–36.
[17] Graham ES, Angel CE, Schwarcz LE, Dunbar PR, Glass M. Detailed characterisation of CB2 receptor protein expression in peripheral blood immune cells from healthy human volunteers using flow cytometry. Int J Immunopathol Pharmacol 2010;23:25–34.
[18] Basu S, Dittel BN. Unraveling the complexities of cannabinoid receptor 2 (CB2) immune regulation in health and disease. Immunol Res 2011;51:26–38.
[19] Mackie K. Cannabinoid receptors as therapeutic targets. Annu Rev Pharmacol Toxicol 2006;46:101–22.
[20] Nagarkatti P, Pandey R, Rieder SA, Hegde VL, Nagarkatti M. Cannabinoids as novel anti-inflammatory drugs. Future Med Chem 2009;1:1333–49.
[21] Millar RP, Newton CL. The year in G protein-coupled receptor research. Mol Endocrinol 2010;24:261–74.
[22] Miller LK, Devi LA. The highs and lows of cannabinoid receptor expression in disease: mechanisms and their therapeutic implications. Pharmacol Rev 2011;63:461–70.
[23] Rozenfeld R. Type I cannabinoid receptor trafficking: all roads lead to lysosome. Traffic 2011;12:12–8.
[24] Wu DF, Yang LQ, Goschke A, Stumm R, Brandenburg LO, Liang YJ, et al. Role of receptor internalization in the agonist-induced desensitization of cannabinoid type 1 receptors. J Neurochem 2008;104:1132–43.
[25] Grimsey NL, Graham ES, Dragunow M, Glass M. Cannabinoid receptor 1 trafficking and the role of the intracellular pool: implications for therapeutics. Biochem Pharmacol 2010;80:1050–62.
[26] Atwood BK, Straiker A, Mackie K. CB2. Therapeutic target-in-waiting. Prog Neuro-Psychopharmacol Biol Psychiatry, doi:10.1016/j.pnpbp.2011.12.001.
[27] Bouaboula M, Dussossoy D, Casellas P. Regulation of peripheral cannabinoid receptor CB2 phosphorylation by the inverse agonist SR 144528. Implications for receptor biological responses. J Biol Chem 1999;274:20397–405.
[28] Derocq JM, Jbilo O, Bouaboula M, Segui M, Clere C, Casellas P. Genomic and functional changes induced by the activation of the peripheral cannabinoid receptor CB2 in the promyelocytic cells HL-60. Possible involvement of the CB2 receptor in cell differentiation. J Biol Chem 2000;275:15621–28.
[29] Carrier EJ, Kearn CS, Barkmeier AJ, Breese NM, Yang W, Nithipatikom K, et al. Cultured rat microglial cells synthesize the endocannabinoid 2-arachidonylglycerol, which increases proliferation via a CB2 receptor-dependent mechanism. Mol Pharmacol 2004;65:999–1007.
[30] Shoemaker JL, Joseph BK, Ruckle MB, Mayeux PR, Prather PL. The endocannabinoid noladin ether acts as a full agonist at human CB2 cannabinoid receptors. J Pharmacol Exp Ther 2005;314:868–75.
[31] Grimsey NL, Goodfellow CE, Dragunow M, Glass M. Cannabinoid receptor 2 undergoes Rab5-mediated internalization and recycles via a Rab11-dependent pathway. Biochim Biophys Acta 2011;1813:1554–60.
[32] Atwood BK, Wager-Miller J, Haskins C, Straiker A, Mackie K. Functional selectivity in CB2 cannabinoid receptor signaling and regulation: implications for the therapeutic potential of CB2 ligands. Mol Pharmacol 2012;81(2):250–63.
[33] Magalhaes AC, Dunn H, Ferguson SS. Regulation of G protein-coupled receptor activity, trafficking and localization by GPCR-interacting proteins. Br J Pharmacol 2012;165(6):1717–36. doi: 10.1111/j.1476-5381.2011.01552.x.
[34] Bohme I, Beck-Sickinger AG. Illuminating the life of GPCRs. Cell Commun Signal 2009;7:16.
[35] Kallal L, Benovic JL. Using green fluorescent proteins to study G-protein-coupled receptor localization and trafficking. Trends Pharmacol Sci 2000;21:175–80.
[36] Liu X, Zweier JL. A real-time electrochemical technique for measurement of cellular hydrogen peroxide generation and consumption: evaluation in human polymorphonuclear leukocytes. Free Radic Biol Med 2001;31:894–901.
[37] de Almeida MC, Silva AC, Barral A, Barral Netto M. A simple method for human peripheral blood monocyte isolation. Mem Inst Oswaldo Cruz 2000;95:221–3.
[38] Pfister TD, Reinhold WC, Agama K, Gupta S, Khin SA, Kinders RJ, et al. Topoisomerase I levels in the NCI-60 cancer cell line panel determined by validated ELISA and microarray analysis and correlation with indenoisoquinoline sensitivity. Mol Cancer Ther 2009;8:1878–84.
[39] Eisen MB, Spellman PT, Brown PO, Botstein D. Cluster analysis and display of genome-wide expression patterns. Proc Natl Acad Sci USA 1998;95:14863–68.
[40] Feyen F, Gertsch J, Wartmann M, Altmann K-H. Design and synthesis of 12-aza-epothilones (azathilones)—non-natural natural products with potent anticancer activity. Angew Chem Int Ed 2006;45:5880–5.
[41] Nievergelt A, Marazzi J, Schoop R, Altmann K-H, Gertsch J. Ginger phenylpropanoids inhibit IL-1β and prostanoid secretion and disrupt arachidonate-phospholipid remodeling by targeting phospholipases A2. J Immunol 2011;187:4140–50.
[42] Park S-A, Kim M-R, Kim P-K, Cho H-D, Han G-Y, Kim C-W. Sample preparation method for plasma membrane proteome analysis. J Chromatogr B 2008;872:177–80.
[43] Cao R, Li X, Liu Z, Peng X, Hu W, Wang X, et al. Integration of a two-phase partition method into proteomics research on rat liver plasma membrane proteins. J Proteome Res 2006;5:634–42.
[44] Yamazaki Y, Nagatsuka Y, Oshima E, Suzuki Y, Hirabayashi Y, Hashikawa T. Comprehensive analysis of monoclonal antibodies against detergent-insoluble membrane/lipid rafts of HL60 cells. J Immunol Methods 2006;311:106–16.
[45] Borner C, Hollt V, Sebald W, Kraus J. Transcriptional regulation of the cannabinoid receptor type 1 gene in T cells by cannabinoids. J Leukoc Biol 2007;81:336–43.
[46] Rock R, Gekker G, Hu S, Sheng W, Cabral G, Martin B, et al. WIN55,212-2-mediated inhibition of HIV-1 expression in microglial cells: involvement of cannabinoid receptors. J Neuroimmune Pharmacol 2007;2:178–83.
[47] Kempf K, Hector J, Strate T, Schwarzloh B, Rose B, Herder C, et al. Immune-mediated activation of the endocannabinoid system in visceral adipose tissue in obesity. Horm Metab Res 2007;39:596–600.
[48] Maresz K, Carrier EJ, Ponomarev ED, Hillard CJ, Dittel BN. Modulation of the cannabinoid CB2 receptor in microglial cells in response to inflammatory stimuli. J Neurochem 2005;95:437–45.

[49] Munro S, Thomas KL, Abu-Shaar M. Molecular characterization of a peripheral receptor for cannabinoids. Nature 1993;365:61–5.
[50] Raduner S, Majewska A, Chen JZ, Xie XQ, Hamon J, Faller B, et al. Alkylamides from Echinacea are a new class of cannabinomimetics. Cannabinoid type 2 receptor-dependent and -independent immunomodulatory effects. J Biol Chem 2006;281:14192–206.
[51] Wager-Miller J, Westenbroek R, Mackie K. Dimerization of G protein-coupled receptors: CB1 cannabinoid receptors as an example. Chem Phys Lipids 2002;121:83–9.
[52] Dainese E, Oddi S, Maccarrone M. Interaction of endocannabinoid receptors with biological membranes. Curr Med Chem 2010;17:1487–99.
[53] Colón-González F, Kazanietz MG. C1 domains exposed: from diacylglycerol binding to protein–protein interactions. Biochim Biophys Acta 2006;1761: 827–37.
[54] Thompson D, Whistler JL. Dopamine D3 receptors are down-regulated following heterologous endocytosis by a specific interaction with G protein-coupled receptor-associated sorting protein-1. J Biol Chem 2011;286: 1598–608.
[55] Tanaka M, Sagawa S, Hoshi J-i Shimoma F, Matsuda I, Sakoda K, et al. Synthesis of anilino-monoindolylmaleimides as potent and selective PKCβ inhibitors. Bioorgan Med Chem Lett 2004;14:5171–4.
[56] Martinez-Outschoorn UE, Lin Z, Trimmer C, Flomenberg N, Wang C, Pavlides S, et al. Cancer cells metabolically fertilize the tumor microenvironment with hydrogen peroxide, driving the Warburg effect: implications for PET imaging of human tumors. Cell Cycle 2011;10:2504–20.
[57] Huyer G, Liu S, Kelly J, Moffat J, Payette P, Kennedy B, et al. Mechanism of inhibition of protein-tyrosine phosphatases by vanadate and pervanadate. J Biol Chem 1997;272:843–51.
[58] Cencioni MT, Chiurchiu V, Catanzaro G, Borsellino G, Bernardi G, Battistini L, et al. Anandamide suppresses proliferation and cytokine release from primary human T-lymphocytes mainly via CB2 receptors. PLoS ONE 2010;5:e8688.
[59] Bari M, Paradisi A, Pasquariello N, Maccarrone M. Cholesterol-dependent modulation of type 1 cannabinoid receptors in nerve cells. J Neurosci Res 2005;81:275–83.
[60] Keren O, Sarne Y. Multiple mechanisms of CB1 cannabinoid receptors regulation. Brain Res 2003;980:197–205.
[61] Kunzelmann-Marche C, Freyssinet J-M, Martínez MC. Loss of plasma membrane phospholipid asymmetry requires raft integrity. J Biol Chem 2002;277: 19876–81.
[62] Xiang Y, Rybin VO, Steinberg SF, Kobilka B. Caveolar localization dictates physiologic signaling of β2-adrenoceptors in neonatal cardiac myocytes. J Biol Chem 2002;277:34280–86.
[63] Pike LJ. Lipid rafts. J Lipid Res 2003;44:655–67.
[64] Kovács P, Pintér M. Effects of phosphoprotein phosphatase inhibitors (phenylarsine oxide and cantharidin) on tetrahymena. Cell Biochem Funct 2001;19:197–205.
[65] Hanke JH, Gardner JP, Dow RL, Changelian PS, Brissette WH, Weringer EJ, et al. Discovery of a novel, potent, and Src family-selective tyrosine kinase inhibitor. J Biol Chem 1996;271:695–701.
[66] Le Gouill C, Parent J-L, Rola-Pleszczynski M, Staňková J. Structural and functional requirements for agonist-induced internalization of the human platelet-activating factor receptor. J Biol Chem 1997;272:21289–95.
[67] Weangsripanaval T, Murota K, Murakami Y, Kominami M, Kusudo T, Moriyama T, et al. Sodium cromoglycate inhibits absorption of the major soybean allergen, Gly m Bd 30 K, in mice and human intestinal Caco-2 cells. J Nutr 2006;136:2874–80.
[68] Carozzi AJ, Ikonen E, Lindsay MR, Parton RG. Role of cholesterol in developing T-tubules: analogous mechanisms for T-tubule and caveolae biogenesis. Traffic 2000;1:326–41.
[69] Willerson JT, Ridker PM. Inflammation as a cardiovascular risk factor. Circulation 2004;109:II-2–10.
[70] Nijsten MW, van Dam GM. Hypothesis: using the Warburg effect against cancer by reducing glucose and providing lactate. Med Hypotheses 2009;73: 48–51.
[71] Benard G, Massa F, Puente N, Lourenço J, Bellocchio L, Soria-Gómez E, et al. Mitochondrial CB1 receptors regulate neuronal energy metabolism. Nat Neurosci, doi:10.1038/nn.3053, in press.
[72] Stern R, Shuster S, Neudecker BA, Formby B. Lactate stimulates fibroblast expression of hyaluronan and CD44: the Warburg effect revisited. Exp Cell Res 2002;276:24–31.
[73] Fischer K, Hoffmann P, Voelkl S, Meidenbauer N, Ammer J, Edinger M, et al. Inhibitory effect of tumor cell-derived lactic acid on human T cells. Blood 2007;109:3812–9.
[74] Lisanti MP, Martinez-Outschoorn UE, Lin Z, Pavlides S, Whitaker-Menezes D, Pestell RG, et al. Hydrogen peroxide fuels aging, inflammation, cancer metabolism and metastasis: the seed and soil also needs fertilizer. Cell Cycle 2011;10:2440–9.
[75] Roiniotis J, Dinh H, Masendycz P, Turner A, Elsegood CL, Scholz GM, et al. Hypoxia prolongs monocyte/macrophage survival and enhanced glycolysis is associated with their maturation under aerobic conditions. J Immunol 2009;182:7974–81.
[76] Pan JG, Mak TW. Metabolic targeting as an anticancer strategy: dawn of a new era? Sci STKE 2007;2007:pe14.
[77] Hsieh C, Brown S, Derleth C, Mackie K. Internalization and recycling of the CB1 cannabinoid receptor. J Neurochem 1999;73:493–501.
[78] Wu D-F, Yang L-Q, Goschke A, Stumm R, Brandenburg L-O, Liang Y-J, et al. Role of receptor internalization in the agonist-induced desensitization of cannabinoid type 1 receptors. J Neurochem 2008;104:1132–43.
[79] Daigle TL, Kwok ML, Mackie K. Regulation of CB1 cannabinoid receptor internalization by a promiscuous phosphorylation-dependent mechanism. J Neurochem 2008;106:70–82.
[80] Martini L, Waldhoer M, Pusch M, Kharazia V, Fong J, Lee JH, et al. Ligand-induced down-regulation of the cannabinoid 1 receptor is mediated by the G-protein-coupled receptor-associated sorting protein GASP1. FASEB J 2007;21:802–11.
[81] Ferguson SSG. Evolving concepts in G protein-coupled receptor endocytosis: the role in receptor desensitization and signaling. Pharmacol Rev 2001;53:1–24.
[82] Sim-Selley LJ. Regulation of cannabinoid CB1 receptors in the central nervous system by chronic cannabinoids. Crit Rev Neurobiol 2003;15:91–119.
[83] Martini L, Thompson D, Kharazia V, Whistler JL. Differential regulation of behavioral tolerance to WIN55,212-2 by GASP1. Neuropsychopharmacology 2010;35:1363–73.
[84] Rozenfeld R, Devi LA. Regulation of CB1 cannabinoid receptor trafficking by the adaptor protein AP-3. FASEB J 2008;22:2311–22.
[85] Schuehly W, Paredes JM, Kleyer J, Huefner A, Anavi-Goffer S, Raduner S, et al. Mechanisms of osteoclastogenesis inhibition by a novel class of biphenyl-type cannabinoid CB(2) receptor inverse agonists. Chem Biol 2011;18: 1053–64.
[86] Sarramegna V, Talmont F, Demange P, Milon A. Heterologous expression of G-protein-coupled receptors: comparison of expression systems from the standpoint of large-scale production and purification. Cell Mol Life Sci 2003;60:1529–46.
[87] Katona I, Sperlágh B, Sík A, Käfalvi A, Vizi ES, Mackie K, et al. Presynaptically located CB1 cannabinoid receptors regulate GABA release from axon terminals of specific hippocampal interneurons. J Neurosci 1999;19:4544–58.
[88] McIntosh HH, Song C, Howlett AC. CB1 cannabinoid receptor: cellular regulation and distribution in N18TG2 neuroblastoma cells. Brain Res Mol Brain Res 1998;53:163–73.
[89] Graham ES, Ball N, Scotter EL, Narayan P, Dragunow M, Glass M. Induction of Krox-24 by endogenous cannabinoid type 1 receptors in Neuro2A cells is mediated by the MEK-ERK MAPK pathway and is suppressed by the phosphatidylinositol 3-kinase pathway. J Biol Chem 2006;281:29085–95.
[90] Leterrier C, Bonnard D, Carrel D, Rossier J, Lenkei Z. Constitutive endocytic cycle of the CB1 cannabinoid receptor. J Biol Chem 2004;279:36013–21.
[91] Brailoiu GC, Oprea TI, Zhao P, Abood ME, Brailoiu E. Intracellular cannabinoid type 1 (CB1) receptors are activated by anandamide. J Biol Chem 2011;286:29166–74.
[92] Leterrier C, Laine J, Darmon M, Boudin H, Rossier J, Lenkei Z. Constitutive activation drives compartment-selective endocytosis and axonal targeting of type 1 cannabinoid receptors. J Neurosci 2006;26:3141–53.
[93] Mackie K. Cannabinoid receptor homo- and heterodimerization. Life Sci 2005;77:1667–73.
[94] Kearn CS, Blake-Palmer K, Daniel E, Mackie K, Glass M. Concurrent stimulation of cannabinoid CB1 and dopamine D2 receptors enhances heterodimer formation: a mechanism for receptor cross-talk. Mol Pharmacol 2005;67: 1697–704.
[95] Ellis J, Pediani JD, Canals M, Milasta S, Milligan G. Orexin-1 receptor-cannabinoid CB1 receptor heterodimerization results in both ligand-dependent and -independent coordinated alterations of receptor localization and function. J Biol Chem 2006;281:38812–24.
[96] Rios C, Gomes I, Devi LA. μ Opioid and CB1 cannabinoid receptor interactions: reciprocal inhibition of receptor signaling and neuritogenesis. Br J Pharmacol 2006;148:387–95.
[97] Carriba P, Ortiz O, Patkar K, Justinova Z, Stroik J, Themann A, et al. Striatal adenosine A2A and cannabinoid CB1 receptors form functional heteromeric complexes that mediate the motor effects of cannabinoids. Neuropsychopharmacology 2007;32:2249–59.
[98] Hájos N, Katona I, Naiem SS, Mackie K, Ledent C, Mody I, et al. Cannabinoids inhibit hippocampal GABAergic transmission and network oscillations. Eur J Neurosci 2000;12:3239–49.
[99] Katona I, Rancz EA, Acsády L, Ledent C, Mackie K, Hájos N, et al. Distribution of CB1 cannabinoid receptors in the amygdala and their role in the control of GABAergic transmission. J Neurosci 2001;21:9506–18.
[100] Balenga NAB, Aflaki E, Kargl J, Platzer W, Schroder R, Blattermann S, et al. GPR55 regulates cannabinoid 2 receptor-mediated responses in human neutrophils. Cell Res 2011;21:1452–69.
[101] Lee SF, Newton C, Widen R, Friedman H, Klein TW. Differential expression of cannabinoid CB(2) receptor mRNA in mouse immune cell subpopulations and following B cell stimulation. Eur J Pharmacol 2001;423:235–41.
[102] Borner C, Hollt V, Kraus J. Activation of human T cells induces upregulation of cannabinoid receptor type 1 transcription. Neuroimmunomodulation 2007;14: 281–6.
[103] Wolfe BL, Trejo J. Clathrin-dependent mechanisms of G protein-coupled receptor endocytosis. Traffic 2007;8:462–70.
[104] Yang C, Kazanietz MG. Divergence and complexities in DAG signaling: looking beyond PKC. Trends Pharmacol Sci 2003;24:602–8.
[105] Yoo SK, Huttenlocher A. Innate immunity wounds burst H_2O_2 signals to leukocytes. Curr Biol 2009;19:R553–5.
[106] Forman HJ. Use and abuse of exogenous H_2O_2 in studies of signal transduction. Free Radic Biol Med 2007;42:926–32.

[107] Antunes F, Cadenas E. Estimation of H_2O_2 gradients across biomembranes. FEBS Lett 2000;475:121–6.
[108] Dröge W. Free radicals in the physiological control of cell function. Physiol Rev 2002;82:47–95.
[109] Reth M. Hydrogen peroxide as second messenger in lymphocyte activation. Nat Immunol 2002;3:1129–34.
[110] Rhee SG, Bae YS, Lee SR, Kwon J. Hydrogen peroxide: a key messenger that modulates protein phosphorylation through cysteine oxidation. Sci STKE 2000;2000:pe1.
[111] Guida M, Ligresti A, De Filippis D, D'Amico A, Petrosino S, Cipriano M, et al. The levels of the endocannabinoid receptor CB2 and its ligand 2-arachidonoylglycerol are elevated in endometrial carcinoma. Endocrinology 2010;151:921–8.
[112] Mustelin T, Vang T, Bottini N. Protein tyrosine phosphatases and the immune response. Nat Rev Immunol 2005;5:43–57.
[113] Tiganis T, Bennett AM. Protein tyrosine phosphatase function: the substrate perspective. Biochem J 2007;402:1–15.
[114] Pitzalis C. Adhesion and migration of inflammatory cells. Clin Exp Rheumatol 1993;11(Suppl. 8):S71–6.
[115] Zhang J, Koh J, Lu J, Thiel S, Leong BSH, Sethi S, et al. Local inflammation induces complement crosstalk which amplifies the antimicrobial response. PLoS Pathog 2009;5:e1000282.